INDUSTRIAL SCIENTIFIC COMPANY
REPORT NO. 233 - 1

February 1954

THE DICHROMATIC RADIATION PYROMETER

William S. Tandler
Richard H. Tourin
Morris Grossman

Industrial Scientific Company

New York 1, N. Y.

Final Report on Contract Nonr 444(00),

Office of Naval Research, Department of the Navy

INDUSTRIAL SCIENTIFIC COMPANY
REPORT NO. 233 - 1

February 1954

THE DICHROMATIC RADIATION PYROMETER

William S. Tandler
Richard H. Tourin
Morris Grossman

Industrial Scientific Company

New York 1, N. Y.

Final Report on Contract Nonr 444(00),

Office of Naval Research, Department of the Navy

FOREWARD

This report was prepared by Industrial Scientific Company, New York 1, N.Y. under U. S. Navy Contract Nonr 444 (00). The contract was administered under the direction of the Power Branch, Office of Naval Research, by Mr. A. G. Lundquist.

ABSTRACT

The DICHROMATIC RADIATION PYROMETER is an instrument for determining temperatures of hot objects, particularly turbine blades and other jet engine parts, by measuring the radiation they emit. The principal feature of this instrument, which distinguishes it from conventional total radiation pyrometers and optical pyrometers, is that the temperature is obtained in terms of the ratio of radiation intensities at two different wavelengths in the emission spectrum of the hot part. By this means, the effects of surface emissivity and ambient conditions, which limit or prevent the use of conventional pyrometers, are eliminated.

The basic principles of the DICHROMATIC PYROMETER were studied theoretically and experimentally, and an experimental instrument was developed and tested. The results obtained in the course of this work led to two main conclusions:

1. The instrument represents a practical approach to temperature measurement in jet engines and in similar applications.

2. Sufficient design data and laboratory experience have been accumulated to begin engineering work on a field instrument for use in engine test and development work.

TABLE OF CONTENTS

LIST OF ILLUSTRATIONS

LIST OF TABLES

THE DICHROMATIC RADIATION PYROMETER

I. INTRODUCTION

The trend toward higher operating temperatures in gas turbines, jet engines, and rockets has imparted increasing importance to the measurement of temperatures of hot engine parts, including turbine blades, and has stimulated interest in new approaches in instrumentation. The conventional method is to attach temperature probes to the parts. This has led to many difficult problems. The difficulties involved in attaching temperature-sensing elements to blades, etc. can be avoided by the use of a radiation method for measuring temperature. However, the conditions prevailing in engines limit the applicability of the conventional optical pyrometers and total radiation pyrometers. The DICHROMATIC RADIATION PYROMETER which forms the subject of this study, represents a new approach, which has been explored in an effort to fill the need for an instrument to obtain accurate measurements of temperatures of engine parts, particularly turbine blade temperatures. The work and the results are described in the following pages. But first, a few remarks on the conventional radiation instruments are in order.

When measuring high temperatures, in cases where contact with the hot object is impractical or undesirable, optical pyrometers and total radiation pyrometers are frequently used.(1) The t o t a l r a d i a t i o n p y r o m e t e r is usable from about 40° C. to the highest temperatures. The range of the o p t i c a l p y r o m e t e r extends upwards only from about 800 deg. C, since below this temperature insufficient luminous radiation is emitted from hot solids for a reading to be taken. These instruments are calibrated against the temperature of a hot object completely enclosed in a region of uniform temperature, such as the interior of a furnace. This is commonly referred to as calibration for blackbody conditions. When measuring temperature of a hot object outside such a homogeneous enclosure, a correction must be made to the reading of the instrument in order to obtain the true temperature. This correction must include the factors of emissivity of the hot surface (2) and absorption of radiation by combustion gases, smoke, etc. Emissivity of the surface depends on the condition of the part and its behavior under intense heat. The absorption depends on the amount, type, and temperature of gases (usually combustion gases) between the instrument and the part.

---

(1) Forsythe, W.E., The Measurement of Radiant Energy (McGraw-Hill Book Co., New York, 1937) p. 355 ff.
(2) loc. cit., p. 379

In practical work where the emissivity and absorption factors are unknown, for example, in a gas turbine, and particularly where they vary with time, the introduction of corrections is not practicable, and accurate measurements cannot be obtained with the conventional optical and radiation pyrometers. In the case of a turbine blade surface, the surface emissivity changes due to oxidation, deposits of fuel residues, etc., and the space between the turbine blade and the measuring instrument is filled with hot combustion gases, which do not have uniform transmission, and which emit radiation of their own. Examples of similar temperature measurement problems are combustion chambers and afterburners in jet engines, metallurgical research involving tests of high temperature materials, and measurements on molten metals. In order to apply radiation methods to measurements of this type, it is necessary to employ a technique which is independent of emissivity, gas transmission, and gas emission. This is not possible with the total radiation pyrometer, nor with the optical pyrometer. A different approach is therefore indicated.

The DICHROMATIC RADIATION PYROMETER makes use of the well-known fact that emission of radiation varies with temperature and this variation is different for different wavelengths in the spectrum of a hot solid. This means that, at any given wavelength, radiant emission changes with temperature. But, in addition, this emission, at any given temperature, varies with the wavelength. If, therefore, one selects two different wavelengths of the spectrum, the ratio of the intensities of emission at these two wavelengths also changes with temperature. This ratio indicates temperature in the DICHROMATIC PYROMETER. The instrument is so designed that it measures radiation at two wavelengths emitted from the same area of the hot object. The emissivity factor is therefore the same for both emission measurements and cancels out in the ratio. The absorption losses cancel also, since both measurements are made over the same optical path. In addition, the two wavelengths used can be chosen in a part of the spectrum where combustion gases are transparent and do not radiate appreciably, so that they do not interfere with the measurement. Thus one of the most important disturbing factors of conventional radiation instruments is eliminated.

Ratio-type instruments, known as "two-color pyrometers" have been described,(3-7) employing optical filters to separate the two

(3) Hottel and Broughton, Ind.Eng.Chem.,Anal.Ed. p. 166 (1932)
(4) G. Maeser, Proc.Inst.Fuel p. s38 (1939)
(5) "Temperature" (Reinhold, New York, 1941) p. 1159
(6) A.I.Dahl and P.D. Freeze, USAF Tech.Rep. 6063 (1950)
(7) A.F.Gibson, J.Sci.Inst. 28, 153 (1951)

wavelengths. While, in principle, the use of filters is an apparently simple means of separating regions of the spectrum, in actuality satisfactory filters are not available. Existing filters do not cover the proper region in the infrared where most of the radiation from hot turbine blades occurs, and it does not seem possible by means of filters to obtain precise definition and separation of two suitable wavelength regions for a ratio instrument. In addition, numerous practical difficulties are involved in the use of filters. The DICHROMATIC RADIATION PYROMETER separates different wavelengths by dispersing the radiation with a prism.

It was the purpose of our program to follow a basic approach in the development of the DICHROMATIC RADIATION PYROMETER. This was carried out first of all by determining suitable wavelengths, bandwidths, and other design parameters in the spectroscopic laboratory. The next phase of the program was the development of an instrument to demonstrate and prove the practicability of the method as such. In fulfilling this task an instrument was designed and built for maximum experimental possibilities. It incorporates an infrared monochromator, so that wavelengths can be selected over a wide range. The optical as well as the mechanical and electronic units also were designed to permit experimentation with various types of apparatus. Finally, the program included extensive laboratory tests, demonstrations and tests of the instrument in the field on a combustion rig, at the Philadelphia Navy Yard. The general conclusions and recommendations of our work are summarized in Section VI. In addition, numerous potential applications of the DICHROMATIC PYROMETER were analyzed, and are described later in this report, under "Applications of the DICHROMATIC PYROMETER".

II. THEORY

Previous treatments of the principle of the DICHROMATIC PYROMETER have invariably been based on the approximate radiation law of Wien. However, the use of Wien's approximation is an unnecessary restriction, since the basic principle of the DICHROMATIC PYROMETER can be derived from more fundamental thermodynamic considerations, as we will show.

To start with, the theoretical basis for the DICHROMATIC PYROMETER follows from the Wien displacement law and Kirchhoff's law. The displacement law may be stated as follows. Consider a source of blackbody radiation in equilibrium at temperature T_1. If the temperature of the blackbody is changed to a different

value T_2, the wavelength of the part of the radiation in the spectral range $d\lambda_1$ at λ_1 is changed to the range $d\lambda_2$ at λ_2 in such a way that

$$\lambda_1 T_1 = \lambda_2 T_2 \quad , \tag{1}$$

and the corresponding spectral brightnesses are related by the expression

$$\frac{J_{\lambda_1}}{J_{\lambda_2}} = \frac{T_1^5}{T_2^5} \quad . \tag{2}$$

In other words the spectral brightness of a blackbody radiator increases with increasing temperature, increasing at a greater rate at shorter than at longer wavelengths.* The corresponding expression for the spectral brightness of a blackbody at temperature T is given by

$$J_\lambda = c_1 \lambda^{-5} f(\lambda T) \quad , \tag{3}$$

where λ is wavelength, T the absolute temperature, c_1 is a constant, and f is some function of the quantity (λT). It follows from the displacement law that for any succession of increasing values of T, we have

---

* For a detailed discussion, see for example Richtmyer and Kennard, Introduction to Modern Physics (McGraw-Hill, New York 1942) p. 154 ff.

$$\frac{dJ_{\lambda_1}}{dT} > \frac{dJ_{\lambda_2}}{dT} \quad , \qquad (4)$$

where $\lambda 1$ and $\lambda 2$ ($\lambda 1 < \lambda 2$) are any two wavelengths. Therefore, the ratio of intensities $J_{\lambda_1}/J_{\lambda_2}$ will be a monotonic function of the temperature.

According to Kirchhoff's law, if one considers a thermal radiator of emissivity e_λ, where $e_\lambda < 1$, its spectral brightness at wavelength λ is given by the product $e_\lambda J_\lambda$. We, therefore can write

$$\frac{e_{\lambda_1} J_{\lambda_1}}{e_{\lambda_2} J_{\lambda_2}} = \frac{e_{\lambda_1} c_1 \lambda_1^{-5} f(\lambda_1 T)}{e_{\lambda_2} c_1 \lambda_2^{-5} f(\lambda_2 T)} \quad , \qquad (5)$$

and, if in addition,

$$e_{\lambda_1} = e_{\lambda_2} \qquad (6)$$

we obtain the relation

$$\frac{J_{\lambda_1}}{J_{\lambda_2}} = \left(\frac{\lambda_2}{\lambda_1}\right)^5 \frac{f(\lambda_1 T)}{f(\lambda_2 T)} \quad . \qquad (7)$$

Equations (4) and (7) form the essential basis for the DICHROMATIC RADIATION PYROMETER.

For practical work both the Wien and Planck forms of the function $f(\lambda T)$ are useful, and these are discussed in detail in Appendix I. However, it should be noted that the validity of the method depends on purely thermodynamic considerations, and not on the form of the function $f(\lambda T)$.

If Wien's approximation is used, the temperature function becomes

$$\frac{J_{\lambda_1}}{J_{\lambda_2}} = \left(\frac{\lambda_2}{\lambda_1}\right)^5 \epsilon^{(c_2/T)\left(\frac{1}{\lambda_2} - \frac{1}{\lambda_1}\right)} \qquad (8)$$

On the other hand, the Planck function leads to the form

$$\frac{J_{\lambda_1}}{J_{\lambda_2}} = \left(\frac{\lambda_2}{\lambda_1}\right)^5 \frac{\left(\epsilon^{c_2/\lambda_2 T} - 1\right)}{\left(\epsilon^{c_2/\lambda_1 T} - 1\right)} \qquad (9)$$

While the theoretical equations serve to elucidate the theory of the DICHROMATIC RADIATION PYROMETER, the design of an instrument does not necessarily involve explicit use of the formulae. Since we know that the ratio of intensities varies monotonically with temperature, it is sufficient to calibrate the instrument against a source of known temperature. On the other hand, if one desires to extend the calibration of the instrument beyond the range possible with a convenient source whose temperature can be determined by other means, then it is necessary to extrapolate the calibration beyond the limits of experimental points. For this purpose the equations derived may be employed. Either the Wien or Planck forms of the function $f(\lambda T)$ may be used, depending upon the accuracy desired.

Even if the theoretical equations are used the calibration of a physical instrument will not usually be absolute. This is due to the fact that the physical instrument measures not the ratio $J_{\lambda_1}/J_{\lambda_2}$ but instead measures the ratio

$$\frac{I_{\lambda_1}}{I_{\lambda_2}} = \frac{\int_{\Delta\lambda_1} \alpha_\lambda J_\lambda d\lambda}{\int_{\Delta\lambda_2} \alpha_\lambda J_\lambda d\lambda} \quad , \tag{10}$$

where I_{λ_1} and I_{λ_2} are the observed outputs of the instrument, $\Delta\lambda_1$ and $\Delta\lambda_2$ are the bandwidths transmitted by the optics, and α_λ is the "transmission factor" of the system. The quantity α_λ incorporates the transmission of the optical system, the sensitivity of the radiation detector, and the gain of the amplifying circuit. For sufficiently small values of $\Delta\lambda_1$ and $\Delta\lambda_2$, J_{λ_1} and J_{λ_2} are nearly constant over the respective bandwidths, and hence equation (10) is approximated very closely by

$$(I_{\lambda_1} / I_{\lambda_2}) = K_{\lambda_1\lambda_2} (J_{\lambda_1} / J_{\lambda_2}) \quad , \tag{11}$$

where

$$K_{\lambda_1\lambda_2} = \alpha_{\lambda_1} \Delta\lambda_1 / \alpha_{\lambda_2} \Delta\lambda_2 \quad .$$

is a constant of the instrument. The shape of the $(I_{\lambda_1}/I_{\lambda_2})$ vs. T curve is therefore the same as that of the $(J_{\lambda_1}/J_{\lambda_2})$ curve. Since the shape of the curve depends only upon the choice of the two wavelengths λ_1 and λ_2, it is sufficient for practical purposes to use a single experimental point to fix the ordinates of the calibration curve; the complete curve is then determined by the theoretical equation. The temperature of the calibrating source should be determined by the methods prescribed for the International temperature scale of 1948.[8]

(8) Stimson, H. F., J. Res. NBS 42, 209 (1949)

Because of the fact that the ratio of intensities at any two wavelengths depends only on the temperature, we have a means of defining a temperature scale for the instrument through the medium of the Planck radiation law, without reference to calibration. The temperatures so defined are then temperatures on the absolute thermodynamic scale, rather than the International scale. The advantage of operating the instrument on such an absolute basis lies in the fact that the system thereby becomes self-contained and requires no reference to an external temperature standard. The use of the DICHROMATIC PYROMETER as an absolute instrument is discussed in Appendix II.

III. EMISSIVITY MEASUREMENTS

In order to determine suitable values of the various parameters involved in the DICHROMATIC RADIATION PYROMETER, as well as to verify the assumptions upon which it is based, a program of experimental measurements was carried out in connection with its design. A high degree of variability was included in the instrument so that many of the quantities involved in its design and operation could be finally determined on the basis of these research results, subsequent to fabrication.

Measurements were made of the infrared emission from samples of turbine blade materials. The measurements were carried out by heating the samples in a furnace and measuring the radiation with an infrared spectrophotometer. Measurements were made over the spectral range 1 to 3 microns, for various spectral bandwidths. These measurements were compared with spectra of other materials of known emissivity, and also with flame spectra.

The relative emissivities of the samples showed little or no variation with wavelength for temperatures up to 2000°F. This confirms the assumption that the emissivity cancels out when we measure the ratio of two intensities, which is one of the basic principles of the DICHROMATIC RADIATION PYROMETER. The measurements are described in detail in Appendix III.

IV. DESCRIPTION OF THE INSTRUMENT

A. Optical System

The DICHROMATIC RADIATION PYROMETER consists essentially of an infrared prism monochromator which has been modified to transmit two wavelengths simultaneously, plus an infrared detector and electrical system, by means of which the ratio of intensities at the two wavelengths can be measured. The complete instrument is shown in Figures 1 and 2.

The prism is made of fused quartz. This material is transparent throughout the 1-3.5 micron range of the infrared spectrum, has high dispersion, is mechanically and chemically stable, and moderate in cost. Detailed data on fused quartz are given in Appendix IV.

In working out the optical system a number of methods of separating the two wavelengths were analyzed. In this connection our design studies emphasized the flexibility required in an experimental or pilot model instrument, rather than attempting to develop the ultimate in a commercial-type instrument. The use of filters was considered, but as has been previously discussed, found unsatisfactory. A basic design question was whether to use a two-wavelength system with a single detector upon which both radiation signals are incident, or two separate detectors, one for each wavelength. The use of two separate detectors was found to produce undesirable complications in the electrical system, as well as difficulties in matching and replacing detectors. It was therefore considered preferable to proceed with a design using a single detector.

The requirements for the detector itself were that it provide high signal-to-noise ratios for the spectral region 1-2.5 microns, that it be rugged and stable in construction, and preferably have a high internal impedance, to permit direct connection to the grid of the amplifier. Moderate speed of responce (up to about 50 cycles) was also a requirement. Two available detectors which meet these requirements are the lead sulfide photoconductive cell and the thermistor bolometer. The lead sulfide cell has the advantage of much higher sensitivity - of the order of 100:1 - than the bolometer in this spectral region; it has the disadvantage as compared to the bolometer of having a high temperature coefficient of sensitivity. Provided that the temperature coefficient is the same for both wavelengths to be used in the Dichromatic instrument, the temperature coefficient is not a serious drawback, since for most practical purposes the effect cancels out in taking the ratio. However,

it was necessary to verify experimentally that the temperature coefficient is not markedly dependent upon wavelength. A series of tests was accordingly conducted to check this point, and the results are described in Appendix V. It was found that the temperature coefficient is, within the accuracy of the measurements, independent of wavelength. This agrees with measurements made by other investigators.(9)

The optical system is shown schematically in Fig. 3 and illustrated in the photograph of Fig. 4. Radiation from the target at A is reflected from the plane mirror M_1, collected by the condensing mirror M2, and focused on the entrance slit S1. The plane mirror M3 is on a sliding amount which can be moved along the track T and interposed in the beam so as to turn it 90 deg. toward the screen SC.

The mirror and screen arrangement is used in alignment for visual sighting on the target; normally the mirror M3 is in the retracted position. To align on the target the entrance window is faced in the direction of the target and the instrument moved until the target is centered in the crosshairs on the screen SC, as seen through the viewing window. For this observation the mirror M3 is pushed forward into the extended position. The distance from M3 to the screen is equal to the distance from M3 to the slit, so that when the target is focused at the former, as judged by visual observation, it is equally focused at the latter when the mirror M3 has been withdrawn to its normal retracted position.

The chopper C is located close to the entrance slit and interrupts light to the upper and lower halves of the slit alternately at a frequency of 13 cycles per second. The mode of operation of the chopper is illustrated in Fig. 5, which shows how the two sector cutouts are located with respect to the slit. The cutouts of the chopper are 180° apart, so that the upper and lower halves of the entrance slit are exposed and masked alternately; since the entrance slit image is inverted by the optical system, the upper and lower halves of the entrance slit itself correspond to the lower and upper halves of the exit slit, respectively.

The precise chopping frequency used is not critical, and 13 cycles was chosen because of the availability of a standard commercial chopper-rectifier unit. The rectifier part of this assembly is a synchronous commutator which consists of a set of three cam-driven breaker points which open and close synchronously with the interruption of the two light beams. The operation of the breakers will be dealt with more fully when their functioning in the electrical

(9) S. H. Duffield, Symposium, Ohio State Univ., June 1952, Paper I 2

system is discussed.

The optical system of the monochromator is that of a Perkin-Elmer Model 83 instrument, with the exception of the split Littrow mirror. Referring once more to Fig. 3, light from the entrance slit illuminates the collimator mirror M4, which in turn fills the prism PR with light. The dispersed beam from the prism is returned by the two halves of the split Littrow mirror and focused on the exit slit by M4 and M5. Light from the exit slit is turned 90° by the small mirror M6 and illuminates the ellipsoid M7. The radiation is condensed by the ellipsoid onto the target surface of the detector, D. The detector is an Eastman Kodak chemically-deposited lead sulfide photoconductive cell.

The split Littrow mirror is illustrated in Fig. 6. The two halves are independently mounted on co-axial shafts in ball bearings. In addition to motion around the ball bearings, the entire assembly can be rotated about the common axis for adjustment purposes. Wavelength settings are made by means of the lever arms which control the rotation of the adjusting shafts. Each lever arm is driven by a Brown & Sharpe micrometer, scales of the micrometers being calibrated for wavelength. The wavelength calibration of the micrometers is given in Fig. 7. By means of the micrometers the wavelengths of the two halves of the Littrow mirror can be set independently. The mirror halves can be tilted from the vertical by means of adjusting screws, which push against spring retainers.

The operation of the system is illustrated in Fig. 8. The angles of the two Littrow mirror halves are adjusted so that wavelength λ_1 is transmitted from the upper half-mirror and wavelength λ_2 is transmitted from the lower half-mirror, both being brought to a focus at the exit slit. The mirror halves are then tilted from the vertical so that the images overlap as shown in the figure. When the upper sector of the chopper is open the upper half of each spectrum image is illuminated, while when the lower sector is in the open position only the lower half of each slit image is illuminated. When neither sector is open both slit images are dark and no light is transmitted to the detector. The upper half of the upper image and the lower half of the lower image are cut off by the adjustable knife edges, so that only the overlapping portions contribute to illuminating the detector. It is evident from the figure that only one of these is illuminated at a time, dependent upon which sector of the chopper is in the open position. Consequently, only one wavelength radiation gets through to the detector at any one time.

Several other methods of separating the two wavelengths were analyzed, and are discussed in Appendix VI. The method used in this

experimental instrument was selected primarily for its simplicity and adaptability, and because it required a minimum of engineering to construct. A more refined design will undoubtedly be necessary for a practical instrument, and this will be discussed later on.

B. Sensitivity and Resolution

The optical unit was designed for a working distance of 4 feet from target to instrument. At this distance an image of the target is projected onto the entrance slit of the instrument reduced to 1/5th actual size. As the full size of the entrance slit is 12 mm high by 0.5 mm wide, the target must be 5 times this size, or 60 mm x 2.5 mm, in order for its image to fill the slit. However, in many applications it is desirable to make measurements on a relatively small area of the hot object. In order to provide for this, a set of adjustable horizontal knife edges were introduced in the entrance slit plane. By means of the knife edges the field of the instrument at the target can be reduced to very small dimensions, so that "spot" temperatures can be obtained.

The smallest area on which the DICHROMATIC PYROMETER can measure is determined by energy considerations. The minimum workable signal to noise ratio required for accurate results is approximately 200:1. In the circuit used in this instrument the detector noise amounts to approximately 50μ-Volts. Thus a signal output from the detector of 10 millivolts is required in order to have 200:1 signal/noise ratio. The sensitivity of the lead sulfide cell varies considerably with operating conditions but on the average a signal of approximately 0.1 μ-watt radiant energy is required in order to obtain 10 millivolts electrical output. The energy received by the detector depends upon the size of the target area viewed, on the temperature of the target, and on the optical aperture of the instrument. In the present instrument an aperture of 80 mm is used. With these optics an area of 0.12 inches by 0.02 inches has been measured satisfactorily at temperatures down to 1000° F. The actual target area in the field of view depends upon the distance of the target from the instrument. In the present case the target was located four feet from the instrument. This resulted in a 1/5 minification of the target area in the optical system, as mentioned above. The area actually surveyed by the instrument was, therefore, 0.6 inches by 0.1 inches.

It is apparent that a variety of combinations of the three factors, - area, optical aperture, and temperature are possible. The functional relations are discussed in Appendix VII. With the present instrument an area at the target as small as 0.04 x 0.04 inches can be measured at a distance of 1 foot for temperatures of 1000° F and up. In general, at larger distances, larger areas are required in order to obtain accurate readings; however, this can be modified by the use of a telescopic sight in conjunction with the instrument.

C. Slitwidth

The DICHROMATIC PYROMETER is used to measure temperatures of solids, and the emission spectrum of a solid radiator is continuous for all wavelengths. Therefore, in determining what slitwidth to use in the monochromator we did not have to consider the question of resolving power, which is ordinarily one of the greatest problems in infrared work.

So far as absorption bands due to combustion gases, etc. are concerned it is desirable that the slits not be so wide as to overlap any portion of these bands. The extent of this limitation is indicated in Fig. 9. This example shows that a slitwidth setting of 0.07μ at wavelength 2.1μ can be used without overlapping the atmospheric absorption bands. A wider slit would result in overlapping of the 2.2μ band, which might result in errors, due to changing humidity.

In general, for a solid radiating source the energy transmitted to the detector is proportional to the square of the slitwidth, as long as the source image fills the slit. Thus there is an advantage to using wide slits, as this enables one to provide ample energy for the detector, thereby obtaining a high signal-to-noise ratio. However, if too wide a slit is used, the wavelengths λ_1 and λ_2 are no longer precisely defined, equation (3) does not apply, and the calibration becomes purely empirical. Since it was desired to avoid this latter condition, measurements of the variation of J_1/J_2 with temperature were made at various slitwidths. As shown, for example, in Fig. 10, the theoretical and experimental curves do not depart appreciably from one another at slitwidths up to 0.4 mm.

In addition to the effect mentioned above there are two other practical limitations on slitwidth. These are the small size (0.2 x 2 mm) of the photocell surface, upon which the radiation must be condensed, and the effect of saturation of the electronic circuit by excessive signal.

In the instrument built under this program saturation is the controlling factor; the widest slit which can be used is that slitwidth at which the system is below saturation for the highest temperature to be measured. Fortunately, for this slitwidth setting at about 2000° F there is still sufficient energy for measurement purposes when the temperature is reduced to 1000°. It is therefore not necessary to change the slitwidth over this range.

The width of the slits has been set in co-ordination with the separation of the adjustable knife edges in order to provide a

compromise between non-saturation of the system at the high temperature end of the scale and adequate signal at the low end. Changing the position of the knife edges changes the amount of radiation received by the instrument for a given temperature of the target, and consequently the slitwidth may have to be changed if the knife edges are re-adjusted.

D. Wavelengths

The wavelengths for the DICHROMATIC PYROMETER were chosen in the following way. In the first place the amount of energy available for the instrument should be as large as possible, and therefore the wavelengths for the instrument should be as close as possible to the peak in the emission spectrum. The location of this peak is dependent upon the temperature, shifting towards shorter wavelengths as the temperature increases. The relative distribution of energy over the spectrum is shown in Fig. 11 for temperatures of 1000° and 2000° F. The next consideration is that the two wavelengths should be spaced sufficiently far apart so that adequate sensitivity is obtained. The criterion for this separation is obtained from equation (8) or (9).

In addition, the selection of the two wavelengths λ_1 and λ_2 is conditioned by the necessity for avoiding atmospheric and flame gas absorption, as well as flame emission. To make this clear the emission spectra of some hydrocarbon combustion gases are shown in Fig. 12. Emission bands occur near 1.9 microns, 2.2 microns, and 2.7 microns in the spectrum, and corresponding absorption bands occur in the atmospheric spectrum. In order to avoid having a large component of gas radiation superimposed on the emission from the turbine blade surface, as well as to avoid distortions produced by fluctuations in the water vapor content of the atmosphere, wavelengths in these absorption bands had to be avoided.

Because of the relatively high concentration of atmospheric absorption bands in the region extending from 2.5 microns towards longer wavelengths, this region was excluded. We therefore had a choice of picking the wavelengths from the ranges 2.35 to 2.51 microns, 1.99 to 2.12 microns, and 1.40 to 1.79 microns. Referring to these regions as 1, 2, 3 respectively, one could choose one of the following combinations: Both wavelengths in 1, both wavelengths in 2, both wavelengths in 3, or pairs of wavelengths in different regions, as 1, 2; 1, 3; 2,3. Of the combinations in which both wavelengths are selected from the same region, only region 3 is sufficiently broad to permit adequate separation, as required by equation (8) or (9). However, the radiation peak does not extend into this region until temperatures over 2400° F are reached, the bulk of the radiation at lower temperatures occurring at the longer

wavelengths. The combination 2, 3 gives a number of choices for the two wavelengths which result in both adequate sensitivity and adequate separation. The combination 1, 2 gives pairs of wavelengths which are too close together, while the combination 1, 3 are too far apart. The choice of one wavelength in the region 2 and one in the region 3 was accordingly felt to be the most satisfactory for the present purpose. The wavelengths ultimately chosen were 1.67 microns in region 3 and 2.10 microns in region 2. This choice of wavelengths provides a variation in the ratio $J\lambda_1/J\lambda_2$ by a factor of about 2.3 over the range 1000° - 2000° F, which compares favorably to the variation of approximately 2 for the emf of a chromel-alumel thermocouple over the same range. The $J\lambda_1/J\lambda_2$ vs. T curve is nearly linear for these wavelengths, which is convenient for setting up a temperature scale. The detailed calculations are given in Appendix VIII.

E. Electronic Circuits.

The signal impinging on the radiation detector consists of alternate pulses at two wavelengths λ_1 and λ_2, each train of pulses modulated at 13 cycles. The detector output therefore consists of a 26-cycle per second electric signal, alternate pulses being of equal magnitude. The output of the preamplifier is fed to the calibrating switch, the cathode follower, volume control step-switch, volume control, and the main amplifier. The circuit arrangement is shown in Fig. 13. The 26-cycle signal output of the final stage of the amplifier is transmitted by way of a differentiating network back to the chopper assembly in the optical unit, and the signal is applied across the breakers of the synchronous commutator. The breakers are driven by cams on the same shaft which drives the chopper, so that the breakers open and close alternately in synchronism with the opening and closing of the sector cut-outs of the chopper. Thus when sector 1, which transmits wavelength λ_1, is open, only breaker 1 conducts, while when sector 2, which transmits only wavelength λ_2, is open, only breaker 2 conducts. In this manner the 26-cycle signal of alternate equal pulses is separated into two 13-cycle signals, each consisting of a train of equal pulses.

The two 13-cycle signals from the breakers are rectified by the 6H6 twin diode. Rectifier I gets the full signal of channel I, and Rectifier II gets a fraction of the signal in channel II determined by the setting of the calibrating control inserted between the breaker and diode II. One of the two signals proceeds by way of the balanced tube voltmeter I. The other signal proceeds by way of the balanced voltmeter II. The volume control step-switch switches the volume level of both signals simultaneously at the input of the amplifier, and the volume control permits continuous adjustment of both signal levels. Varying the amplifier gain does not vary the relationship between the two signals. Therefore, if the gain is adjusted so that one meter always reads the same

value, the reading of the other meter is proportional to the ratio, and its scale can be calibrated in terms of temperature. The constant reading channel is used as a null indicator, and a Brown potentiometer-recorder is used to provide an expanded scale for the reading of the other meter. The tube voltmeter I serves to indicate the signal in channel I, so that the common volume control can be adjusted to keep the indication of voltmeter I constant for all temperatures. Fig. 13 indicates an automatic volume control for this function, although it is being done manually at present. The output of the balanced tube voltmeter II is, on one side, led through the servo-amplifier input terminals to the slide of the self-balancing potentiometer R_p and, on the other side, to the slide of the temperature range potentiometer R_c. One end of the self-balancing potentiometer R_p is connected to one end of this temperature range potentiometer R_c and the other end of R_p is connected to one end of the temperature range resistance R_s. The other ends of R_c and R_s are connected to the source of a balancing potential E_o. The servo-motor indicator moves the slide of R_p to such a position that the current through the servo-amplifier input terminals becomes zero.

The "calibrating switch" permits connecting to the input of the cathode follower either the signal from the detected radiation or a "test" signal derived from the "test signal generator." When the test signal is on, the signal generator supplies equal signals to both channels. The test signal is, therefore, equivalent to that temperature for which the radiation received by the PbS cell is exactly equal for both spectral wavelengths. Whether or not the measured spectral intensities are equal depends on the optical alignment. If the optical and electronic alignment are correct, the test signal can be used to adjust the output of tube voltmeter II by means of the "calibrating control" to the correct value relative to tube voltmeter I, or to set the self-balancing potentiometer to the correct point on its temperature scale, corresponding to unity ratio for the two input signals. If the optical alignment should not be correct, then the calibrating control can be used to compensate for optical misalignments.

The circuits are described in detail in Appendix IX.

F. Calibration

The instrument was calibrated over the range 1000° - 1350° F by sighting it on a blackened iron wedge heated in a small furnace. The temperature of the wedge was measured by means of a calibrated thermocouple. For the range 1350° - 2000° F the Pyrometer was sighted on a globar radiator, the temperature of which was measured by an optical pyrometer. Results of the calibration are shown in Fig. 14. The calibration is believed to be accurate within $\pm$ 7° F over the range 1000° - 2000° F.

Slight changes in the signal intensity from that used during calibration are unimportant since these do not affect the ratio. However, a differential change of sensitivity between the two signal channels, either optical or electrical, has the effect of multiplying the instrument calibration by a constant factor. In order to guard against this source of error the following adjustment has been provided. The lower micrometer of the split Littrow mirror is set to transmit 2.10 micron radiation. The upper micrometer is normally set to transmit 1.67 micron radiation. For checking, the upper micrometer can also be set to 2.10 microns. When this is done, the two signals should be equal, independent of the temperature. This provides a check on differential misalignment. If the two signals are not equal, as indicated by the meters on the amplifier chassis, proper adjustment can easily be made by adjusting the differential gain control until the two signals are once more equal. If the temperature of the target is variable, the criterion in this test is that the two signals, when the wavelengths have been set equal, remain equal when the temperature of the target is varied. This provides a positive check on the alignment of the instrument. It is well to repeat that only a differential misalignment can have any affect on the calibration. This is an advantage peculiar to a ratio type instrument.

V. FIELD TESTS OF DICHROMATIC RADIATION PYROMETER

During the summer of 1953 the DICHROMATIC PYROMETER was set up and operated in the Aeronautical Engine Laboratory of the Naval Air Experimental Station, Philadelphia Navy Yard.* The test facility used in this work consisted of a single burner of the turbojet type installed on a horizontal axis, about 4 ft. off the floor. The burner used aviation gasoline as fuel. An inconel specimen approximately 5" x 1-1/2" was set up downstream of the burner and heated by the flame exhaust of the burner. Sixteen thermocouples were arranged in four rows on the specimen, as shown in Figure 15. The specimen was exposed to view on the side opposite from the thermocouple leads, and the DICHROMATIC PYROMETER was sighted on areas of the surface of this side of the specimen. The burning was quite turbulent and uneven so that pronounced

* These facilities were made available by courtesy of the Bureau of Aeronautics, Navy Department. The tests were carried out in co-operation with NAES personnel, under supervision of Mr. J. A. Telerico and Mr. A. T. Murri.

temperature gradients existed across the surface of the specimen.

For these tests the optical unit of the DICHROMATIC PYROMETER was mounted on a rotary table, which was bolted down upon a portable elevator table, as shown in Fig. 1. The instrument was aligned on the target by sighting so as to obtain an image of the target area in the crosshairs of the viewing screen. The calibration settings of the instrument were checked against the internal standard signal, by the method previously described.

The first data obtained are shown in Table I, where the thermocouple readings and DICHROMATIC PYROMETER readings are compared. The measurements were also checked against a standard optical pyrometer. Study of the data obtained in the first tests indicated that the measurements were affected by the very large temperature gradient along the specimen, existing in the vertical direction due to uneven burning. The gradient had an effect on the correlation between thermocouple readings and DICHROMATIC PYROMETER readings, since the DICHROMATIC PYROMETER was measuring over a larger area than the thermocouple. In addition, the temperature distributions measured with the thermocouples showed considerable variation. This is illustrated in Figure 16, where the temperature difference between two adjacent thermocouples has been plotted against the average of their readings. It appears from this that the temperature distribution over the actual target area was not always the same for the same average indicated thermocouple temperature. As a result, certain differences between thermocouple and pyrometer readings must be expected. On the other hand, the gradient in the streamline direction, at any height, was much less than the vertical gradient. Therefore, it was clear that a rotation of the instrument by 90° would provide target areas of substantially more uniform temperature.

In accordance with the above finding a new mount was provided by NAES which enabled mounting the instrument in a vertical position. The position of the target area viewed by the instrument is shown in Fig. 17, which indicates the effect of this change. The change in mounting necessitated elimination of the adjustable rotary table previously used in alignment; after this, adjustments in alignment were made by moving the elevator table. Although the instrument had been designed for operation in a horizontal position, its rigid construction permitted it to be operated vertically without apparent impairment of its performance. The only change made in the instrument was the provision of a metal cover over the exposed chopper assembly, to prevent damage and to minimize the entry of dirt.

Following installation of the instrument in the vertical position it was re-aligned on the target and additional measurements made.

These measurements extended over the latter part of June and early July. The data obtained are summarized in Table II. The data taken up to July 9th, as given in Tables I and II, have been summarized in Figure 18. The points corresponding to higher and lower temperatures during a given run lie on a smooth curve, and runs taken within a short time of one another are in agreement. However, considering the data taken over the entire period, it is apparent that inconsistencies exist among runs made at various times.

At this point the instrument was demonstrated to personnel of the Bureau of Aeronautics, and a meeting was held of representatives of the Bureau, N.A.E.S., and Industrial Scientific Company. It was agreed that in order to show the applicability of the DICHROMATIC PYROMETER to problems of temperature measurement in the field it was necessary to demonstrate reliable, reproducible results. In order to carry out this purpose the program of measurements was continued as described below. First, some time was devoted to obtaining additional data, without changing the operating conditions, in order to re-check the data previously obtained. Much the same results were obtained as before: measurements taken over several repeated runs agreed well with one another, but curves obtained several days or weeks apart showed certain deviations from one another.

Following these additional measurements, a check was made of the alignment and operation of both the electrical and optical components of the instrument. During this period a switch was added to the circuit to the circuit to permit transferring the signal in Channel II over to Channel I, thus making it possible to read both signals on the same meter.

A further series of tests were made to investigate possible effects of optical misalignment. It was found that small deflections of the instrument with respect to the target had no appreciable effect in disturbing the calibration. During this work we found it possible to reduce the aperture of the instrument to approximately 1/2 of its original setting. For this purpose the adjustable knife edges were moved closer together. The reduction of aperture further minimized possible effects of misalignment and also reduced the temperature gradient in the target area, by making this area smaller.

After these adjustments and checks had been made the following procedure was adopted: a globar * radiator was mounted on the burner assembly, in a position such that the DICHROMATIC PYROMETER could be sighted on either the globar or the test specimen without any adjustment other than changing the height of the elevator table. This permitted frequent checking of the pyrometer scale against the

---

* The globar is a silicon carbide rod about 1-1/2" long and 1/4" in diameter, which is heated by passing an electric current through it.

globar. Using this arrangement, a series of temperature runs was made during September. The data obtained are given in Table III, and are plotted in Figure 19. It is apparent that the reproducibility of the measurements over short periods of time, as well as the long-time stability, were both greatly improved compared to the earlier data. In these measurements the mean deviation of immediately following runs was within better than $\pm$ 1%, while the mean deviation of the whole set of runs was within $\pm$ 2% of full scale. These results indicate that the method is inherently capable of good precision.

VI. SUMMARY AND RECOMMENDATIONS

It was the purpose of the present project to explore the practical applicability of the DICHROMATIC radiation method of measuring temperatures of hot solids. In the course of this exploratory study and as part of the project, the present instrument was built, subjected to extensive tests, and demonstrated in operation. In order to fulfill this basic concept of exploration and test, particular attention was paid to construction of the instrument for experimental purposes. In fact, it was the very idea of being able to experiment not only with the instrument as a whole but with individual components which directed our design.

Inasmuch as no instrument of this type had been built before, our approach had to be basic, and the first task was to design and build an instrument which in the quickest possible way and with the least amount of complications could clarify the basic facts and the workability of the method. We succeeded in establishing the theoretical foundation of our work within a relatively short time after its inception, and we could then proceed to the investigation of components as well as allover layout.

Because previous experience was limited, it was necessary to try and test a variety of mechanical, optical, and electrical components, and combinations. The simple and box-like construction of our instrument and the design for interchangeability facilitated this work. After the basic principles had been checked out we proceeded to various refinements, to the degree that we could predict their results and check them in our own laboratory. This being done, we proceeded to the next step of testing the DICHROMATIC PYROMETER in the field, at the Philadelphia Navy Yard. This part of the program was carried out together with personnel of the Naval Air Experimental Station, to whom thanks are due for their co-operation, and help and advice on many occasions.

In the course of this work, the construction for strictly experimental purposes proved its value, and made it possible to make all adjustments on the spot, as they were indicated in the field work. This procedure, of strictly applying experimental expediency and following the principle of attaining conclusive experimental results first instead of aiming at ultimate perfection, paid off. The instrument worked from the very beginning and delivered experimental data. Various difficulties were encountered and overcome as described above. The test results were interpreted and analyzed as the work progressed. Improvements were made, and finally good performance of the instrument as a whole was achieved.

Naturally such a procedure, while leading in our opinion in the fastest and most direct way to a conclusive picture of the problem and its solution, does not, by necessity, concern itself with what is called "final design". In fact, this was not the purpose of the project. However, the experience gained was broad and conclusive, and in the later stages of our work it became quite clear that a definitive instrument for practical field purposes, and beyond what our experimental instrument had already shown, could be designed and built. Also, a great number of data could be accumulated which would make the design and the construction of a field instrument substantially an "engineering job". In other words, we believe that our research and development activity has progressed far enough to start with the final engineering, requiring, as far as the instrument itself is concerned, only a small amount of research. On the other hand the phenomena observed and many other considerations indicate that independent of the work on a field instrument, a considerable variety of scientific tasks can be envisaged in which the experience gained during this project, as well as the actually existing "experimental instrument" could be utilized with great advantage.

The experimental instrument in several ways could be used "as is". However, a certain amount of rebuilding and improvement would certainly be advisable. The list of our suggestions in this respect closely matches the recommendations for a new or field instrument, and we list these recommendations herebelow with the thought that they could be used both for reconditioning of the experimental instrument and as a guide and basis for a field instrument. The major points are outlined below. Many of the smaller points can be gleaned from the details elaborated in the pages of this report.

1. As discussed in Section IV, the present instrument is operated by manually controlling the amplifier gain to maintain the signal in one channel stationary. The temperature reading is then given by the deflection of the meter of the second channel.

An automatic servo system to replace this manual adjustment would be desirable. Besides being more accurate, convenient, and rapid, this would permit c o n t i n u o u s r e c o r d- i n g of temperatures.

2. The present system uses a split optical system, consisting of two parallel channels, one half the radiation received from the target being used in each channel. This arrangement was of major advantage because of its experimental flexibility. However, the resolving power, stability and a number of other features could be considerably improved. While various ways of effecting these changes are possible, their purpose is to use a single path method, in which both channels coincide, instead of the split system of the experimental unit. This can be done in several ways, mainly by changes in the optical system and the chopper arrangement.

3. The electrical system requires refinement. Both linearity and stability of the amplifiers can no doubt be improved. The scale of the instrument, now in arbitrary numbers, could read the ratios and their corresponding temperatures directly.

4. The alignment of the instrument on the target by means of the ground glass screen proved satisfactory, but could be refined.

5. The present instrument is very ruggedly built and is usable in almost any position. As an experimental device its size was not considered important. However, it seems desirable to reduce the size of the instrument in order to make it easier to handle, and this could be readily done.

VII. APPLICATIONS OF THE DICHROMATIC RADIATION PYROMETER

The redesigned instrument discussed above would be a definitive DICHROMATIC PYROMETER for measuring temperatures at distances up to about 6 feet. For measurements over long distances, above 6 feet, for which numerous applications can be visualized, the same instrument can be used, with the addition of an optical system, (a telescopic sight). In the course of this project such a sight has been investigated and found readily feasible for measurements up to at least 30 feet.

The DICHROMATIC PYROMETER is useful for measuring temperature in many instances where other instruments are not satisfactory.

Some of the many applications are the following:

1. Turbine blades, etc.
2. Afterburner and tailpipe wall temperatures in jet engines.
3. Tailcone temperatures.
4. Temperatures of melts of unknown emissivity.
5. Temperature measurements in smoky or dusty atmospheres.
6. Furnace wall temperatures where the optical path goes through flame gas.
7. Temperatures in the interior of steam turbines.

One of the important applications envisaged for the DICHROMATIC RADIATION PYROMETER has been the measurement of temperatures of moving parts, particularly turbine blades in rotation. For these applications some supplementary equipment may be necessary in addition to the instrument itself. Also a number of possibilities have been worked out to closely localize the measurement on particular sections of the rotating member. We wish to explain this by means of two illustrative examples.

Fig. 20 shows a rotating turbine wheel on a turbosupercharger. When viewed in the position shown, the blades of the turbine wheel form a continuous surface from which radiation is being emitted at every point. In this figure the small solid rectangle shows the area on the turbine wheel which is viewed by the instrument at any particular time. The shaded arc shows the area swept out in the field of view of the instrument as the turbine rotates. The width of this ring can be made extremely small, of the order of 1 mm. The radial distance may be varied by moving the instrument and sighting on different points. The precise location sighted can be observed on the viewing screen of the instrument. In this arrangement it is possible to measure temperatures at various distances along the blades from the root out to the tip.

Another example is the measurement of temperatures of blades in a gas turbine, assuming that measurement is being made from the tail end of the turbine, i.e., through the tailpipe opening. (An alternative would be to make the measurement through an opening in the side of the turbine wall.) In this case it is possible to sight on the turbine blades by the following device. A rotating chopper can be introduced at some convenient point so as to interrupt the radiation beam coming from the blades. This chopper

can be synchronized with the rotation of the turbine, through the turbine takeoff, so that the beam can be cut off whenever the blades of the rotor are not in view, while the chopper permits radiation to pass when sections of the blades are presented to the field of view. This scheme may be extended so as to localize sections along the radius of the blades, and to permit measurement on less than the full number of blades. Thus the possibility exists of measuring temperatures not just along circumferential strips, as discussed in the previous example, but also at particular points on the blades, and on selected blades. A number of installations exist where a clear view into the tailpipe is available, so that this technique could be applied.

APPENDIX I. APPLICATION OF THE RADIATION LAWS TO THE DICHROMATIC RADIATION PYROMETER

If the Wien approximate radiation law is used, then an upper limit is imposed on the range of temperature which can be measured with the DICHROMATIC RADIATION PYROMETER.

This may be understood as follows. For any small wavelength interval $d\lambda$, the spectral brightness is given exactly by the Kirchhoff-Planck relation

$$e_\lambda J_\lambda d\lambda = e_\lambda c_1 \lambda^{-5} \left(\epsilon^{c_2/\lambda T} - 1\right)^{-1} d\lambda, \qquad (I.1)$$

where e_λ is the spectral emissivity at wavelength λ, c_1 and c_2 are the radiation constants, and T is the absolute temperature. Then for any two wavelengths λ_1 and λ_2 we have

$$\frac{e_{\lambda_1} J_{\lambda_1} d\lambda_1}{e_{\lambda_2} J_{\lambda_2} d\lambda_2} = \frac{e_{\lambda_1}}{e_{\lambda_2}} \left(\frac{\lambda_2}{\lambda_1}\right)^5 \frac{\left(\epsilon^{c_2/\lambda_1 T} - 1\right) d\lambda_1}{\left(\epsilon^{c_2/\lambda_2 T} - 1\right) d\lambda_2} \qquad (I.2)$$

If the factors of unity in the parentheses are dropped and we assume $e_{\lambda_1} = e_{\lambda_2}$, we obtain the approximation

$$\frac{J_{\lambda_1} d\lambda_1}{J_{\lambda_2} d\lambda_2} = \left(\frac{\lambda_2}{\lambda_1}\right)^5 \epsilon^{(c_2/T)\left(\frac{1}{\lambda_2} - \frac{1}{\lambda_1}\right)} . \qquad (I.3)$$

The approximation is accurate to within 1% in J_λ, provided that the product λT does not exceed 0.3 cm-deg. This equation can be solved explicitly for T, and one gets

$$T = \frac{c_2 (\lambda_1 - \lambda_2)}{\lambda_1 \lambda_2 \log_\epsilon \left[\frac{J_{\lambda_1} d\lambda_1}{J_{\lambda_2} d\lambda_2} \left(\frac{\lambda_1}{\lambda_2}\right)^5 \frac{d\lambda_2}{d\lambda_1}\right]} \qquad . \qquad (I.4)$$

A more exact formulation can be obtained if we omit the simplification used above and retain the factors of unity in the parentheses.

The ratio of radiant intensities at two different wavelengths λ_1 and λ_2 is then obtained by setting $e_{\lambda_1} = e_{\lambda_2}$ in equation (I.2), and in place of equation (I.3), we get

$$\frac{J_{\lambda_1} d\lambda_1}{J_{\lambda_2} d\lambda_2} = \left(\frac{\lambda_2}{\lambda_1}\right)^5 \frac{\epsilon^{c_2/\lambda_2 T} - 1}{\epsilon^{c_2/\lambda_1 T} - 1} \frac{d\lambda_1}{d\lambda_2} \qquad (I.5)$$

Another expression for the ratio $J_{\lambda_1}/J_{\lambda_2}$ in terms of T can be obtained as follows. First we write

$$\epsilon^{c_2/\lambda T} = 1 + e_\lambda c_1 \lambda^{-5}/J_\lambda \qquad (I.6)$$

so that

$$\exp\left[\frac{c_2}{T}\left(\frac{1}{\lambda_2} - \frac{1}{\lambda_1}\right)\right] = \frac{1 + e_{\lambda_2} c_1 \lambda_2^{-5}/J_{\lambda_2}}{1 + e_{\lambda_1} c_1 \lambda_1^{-5}/J_{\lambda_1}}$$

$$= \frac{J_{\lambda_2} + e_{\lambda_2} c_1 \lambda_2^{-5}}{J_{\lambda_1} + e_{\lambda_1} c_1 \lambda_1^{-5}} \frac{J_{\lambda_1}}{J_{\lambda_2}}. \qquad (I.7)$$

Upon taking the natural logarithms of both sides we obtain

$$\frac{c_2}{T}\left(\frac{1}{\lambda_2} - \frac{1}{\lambda_1}\right) = \log_\epsilon \frac{J_{\lambda_1}}{J_{\lambda_2}} + \log_\epsilon \left[\frac{J_{\lambda_2} + e_{\lambda_2} c_1 \lambda_2^{-5}}{J_{\lambda_1} + e_{\lambda_1} c_1 \lambda_1^{-5}}\right], \qquad (I.8)$$

which can be solved for $\log_\epsilon \left(J_{\lambda_2}/J_{\lambda_1}\right)$, to give

$$\log_\epsilon \left(J_{\lambda_2}/J_{\lambda_1}\right) = \frac{c_2}{T}\left(\frac{1}{\lambda_2} - \frac{1}{\lambda_1}\right) + \log_\epsilon \left[\frac{J_{\lambda_2} + e_{\lambda_2} c_1 \lambda_2^{-5}}{J_{\lambda_1} + e_{\lambda_1} c_1 \lambda_1^{-5}}\right]. \qquad (I.9)$$

Solving equation (I.9) for T we obtain

$$T = \frac{c_2[(1/\lambda_2)-(1/\lambda_1)]}{\log_e(J_{\lambda_2}/J_{\lambda_1})-\log_e(J_{\lambda_2}+e_{\lambda_2}c_1\lambda_2^{-5}/J_{\lambda_1}+e_{\lambda_1}c_1\lambda_1^{-5}}$$

The error incurred in using Wien's formula can be obtained as follows.

From a previcus equation we have, approximately,

$$J_\lambda = e_\lambda c_1 \lambda^{-5} \epsilon^{-c_2/\lambda T} \quad . \tag{I.10}$$

In the same manner as was used above we can show that

$$\log\left(\frac{J_{\lambda_2}}{J_{\lambda_1}}\right) = A/T + \log \frac{e_{\lambda_2}}{e_{\lambda_1}}\left(\frac{\lambda_1}{\lambda_2}\right)^5 . \tag{I.11}$$

Since $e_{\lambda_1} = e_{\lambda_2}$, the above formula becomes

$$\log(J_2/J_1) = A/T + B \tag{I.12}$$

where

$$A = c_2\left(\frac{1}{\lambda_2} - \frac{1}{\lambda_1}\right)$$

$$B = 5\log(\lambda_1/\lambda_2) \tag{I.13}$$

The graph of $\log (J\lambda_2/J\lambda_1)$ vs. $1/T$ is a straight line.

Thus a measurement of $J\lambda_2/J\lambda_1$ determines the value of T. The relative error involved in using Wien's law will be given by

$$\Delta E = \frac{\log(J_{\lambda_2}/J_{\lambda_1})_P - \log(J_{\lambda_2}/J_{\lambda_1})_W}{\log(J_{\lambda_2}/J_{\lambda_1})_P} , \tag{I.14}$$

where the subscripts W and P refer to the values of the ratios using the Wien and Planck laws respectively. From equations (I.9) and (I.12) equation (I.14) can be written

$$\Delta E = \frac{\log \frac{J_{\lambda_2} + e_{\lambda_2} c_1 \lambda_2^{-5}}{J_{\lambda_1} + e_{\lambda_1} c_1 \lambda_1^{-5}} + B}{\log (J_{\lambda_2} / J_{\lambda_1})} \qquad \text{(I.15)}$$

The term

$$\log \frac{J_{\lambda_2} + e_{\lambda_2} c_1 \lambda_2^{-5}}{J_{\lambda_1} + e_{\lambda_1} c_1 \lambda_1^{-5}}$$

can be written in a more instructive form as follows. From Planck's law it becomes

$$\log \left[\frac{e_{\lambda_2} c_1 \lambda_2^{-5} (\epsilon^{c_2/\lambda_2 T} - 1)^{-1} + e_{\lambda_2} c_1 \lambda_2^{-5}}{e_{\lambda_1} c_1 \lambda_1^{-5} (\epsilon^{c_2/\lambda_1 T} - 1)^{-1} + e_{\lambda_1} c_1 \lambda_1^{-5}} \right]$$

$$= \log \left\{ \frac{e_{\lambda_2}}{e_{\lambda_1}} \left(\frac{\lambda_1}{\lambda_2} \right)^5 \left[\frac{(\epsilon^{c_2/\lambda_2 T} - 1)^{-1} + 1}{(\epsilon^{c_2/\lambda_1 T} - 1)^{-1} + 1} \right] \right\} .$$

If $e_{\lambda_1} = e_{\lambda_2}$, the above quantity becomes

$$5 \log (\lambda_1 / \lambda_2) + \log \left[\frac{(\epsilon^{c_2/\lambda_2 T} - 1)^{-1} + 1}{(\epsilon^{c_2/\lambda_1 T} - 1)^{-1} + 1} \right]$$

$$= B + \log \frac{(\epsilon^{c_2/\lambda_2 T} - 1)^{-1} + 1}{(\epsilon^{c_2/\lambda_1 T} - 1)^{-1} + 1} .$$

Hence the percent error is

$$\Delta E = \frac{\log \left[(\epsilon^{c_2/\lambda_2 T} - 1)^{-1} + 1 \right] / \left[(\epsilon^{c_2/\lambda_1 T} - 1)^{-1} + 1 \right]}{\log (J_{\lambda_2} / J_{\lambda_1})_P} \qquad \text{(I.16)}$$

We now consider the effect of an error in log $(J_{\lambda_2}/J_{\lambda_1})$ on the temperature measurement. Suppose the true temperature is given by

$$\log(J_{\lambda_2}/J_{\lambda_1}) = A/T + B + D. \tag{I.17}$$

If we use the Wien's law value of log $(J_{\lambda_2}/J_{\lambda_1})$, equation (I.12), we can find the relation between an error in $(J_{\lambda_2}/J_{\lambda_1})$ and an error in T.

We have

$$\Delta\left[\log(J_{\lambda_2}/J_{\lambda_1})\right] = -(A/T^2)\Delta T \tag{I.18}$$

or

$$\Delta T = -T^2/A\ \Delta\left[\log(J_{\lambda_2}/J_{\lambda_1})\right]. \tag{I.19}$$

We can take $\Delta\left[\log(J_{\lambda_2}/J_{\lambda_1}\right]$ equal to D in equation (I.17), which is, if Planck's law gives the true value of $\log(J_{\lambda_2}/J_{\lambda_1})$,

$$D = \log \frac{\left(\epsilon^{c_2/\lambda_2 T} - 1\right)^{-1} + 1}{\left(\epsilon^{c_2/\lambda_1 T} - 1\right)^{-1} + 1} \tag{I.20}$$

Hence equation (I.19) becomes

$$T = -\frac{T^2}{A} D \tag{I.21}$$

The percent error in T is $\Delta T/T$, so

$$\frac{\Delta T}{T} = -\frac{T}{A} D. \tag{I.22}$$

For a temperature measuring device accurate to within 1% we must have

$$\frac{\Delta T}{T} \leq 0.01 \ .$$

Substituting the value T = 1500° K, we have D = 0.01, A = 1930, so that

$$\frac{\Delta T}{T} = \frac{1500 \times 0.01}{1930} = 0.778\% \ ,$$

which means the error is less than 1% for this particular case.

APPENDIX II. THE DICHROMATIC RADIATION PYROMETER AS AN ABSOLUTE INSTRUMENT.

The absolute nature of the DICHROMATIC RADIATION PYROMETER may be understood as follows. Using the Planck form for $f(\lambda T)$ in equation (3), and substituting into equation (11), we have that the ratio of measured intensities at any two wavelengths λ_1 and λ_2 is given by

$$\frac{I_{\lambda_1}}{I_{\lambda_2}} = \frac{\lambda_1^{-5}\left(\epsilon^{c_2/\lambda_1 T} - 1\right)^{-1} \Delta\lambda_1 \alpha_{\lambda_1}}{\lambda_2^{-5}\left(\epsilon^{c_2/\lambda_2 T} - 1\right)^{-1} \Delta\lambda_2 \alpha_{\lambda_2}} \ . \qquad \text{(II.1)}$$

If $\lambda 1 = \lambda 2$ then the Planck functions cancel in equation (II.1) and $\Delta\lambda_1 = \Delta\lambda_2$; then equation (II.1) reduces to

$$\left(I_{\lambda_1} / I_{\lambda_2}\right)_{\lambda_1 = \lambda_2} = \left(\alpha_{\lambda_1} / \alpha_{\lambda_2}\right)_{\lambda_1 = \lambda_2} \ . \qquad \text{(II.2)}$$

In general

$$\alpha_{\lambda_1} \neq \alpha_{\lambda_2}$$

for a physical instrument, even for $\lambda_1 = \lambda_2$, and therefore

$$\left(I_{\lambda_1} / I_{\lambda_2}\right)_{\lambda_1 = \lambda_2} \neq 1 \quad . \tag{II.3}$$

However, we may assume that the physical instrument can be adjusted so that its sensitivity to radiation of wavelength λ_1 is equal to its sensitivity to radiation of wavelength λ_2. When this adjustment has been made then $\alpha_{\lambda_1} = \alpha_{\lambda_2}$ and we may speak of the system as having been "normalized". Under this condition, the ratio $\alpha_{\lambda_1} / \alpha_{\lambda_2}$ cancels from equation (II.1) and we have, for $\lambda_1 = \lambda_2$

$$\left(I_{\lambda_1} / I_{\lambda_2}\right) = \left(J_{\lambda_1} / J_{\lambda_2}\right)\left(\Delta\lambda_1 / \Delta\lambda_2\right) \tag{II.4}$$

Here I_{λ_1} and I_{λ_2} are the readings of the instrument, while J_{λ_1} and J_{λ_2} are the spectral brightnesses in absolute units. Solving for the absolute ratio $J_{\lambda_1}/J_{\lambda_2}$, we have

$$\left(J_{\lambda_1} / J_{\lambda_2}\right) = \left(I_{\lambda_1} / I_{\lambda_2}\right)\left(\Delta\lambda_2 / \Delta\lambda_1\right) \tag{II.5}$$

The ratio $I_{\lambda_1}/I_{\lambda_2}$ is the quantity indicated by the instrument after normalization; the bandwidths can be calculated from the dispersion data; this is discussed in Appendix IV. The temperature scale of the instrument can then be calculated from equation (II.4) together with equation (9).

APPENDIX III. EMISSIVITIES OF TURBINE BLADE MATERIALS.

The setup used in the radiation measurements is illustrated in Fig. 21. Fig. 22 is a diagram of the experimental arrangement. The furnace used was a 2-1/2" inside diameter refractory tube 16" long, which could be heated to 2000° F by passing current through a heavy nichrome coil wound upon it. The furnace temperature was monitored by a chromel-alumel thermocouple, the output of which was measured by a Foxboro potentiometer-controller. The temperatures in the furnace could be maintained constant to within ± 2° F. Power was supplied by a 1000 watt variable transformer. Temperatures of the samples were measured by attached chromel-alumel thermocouples. The thermocouples were calibrated against a standard thermocouple, and their temperatures indicated on a Foxboro potentiometer-indicator. The standard thermocouple and the potentiometer-indicator were calibrated by the National Bureau of Standards. Calibration of the thermocouples is described in Appendix X.

The setup functions as follows. Referring to Fig. 22, radiation from the sample in the furnace at A is collected by the spherical mirror M_1, reflected by the plane mirror M_2 and imaged at point P. A motor-driven sector disc interrupts the light beam at P to produce a modulated signal for AC amplification. The point P is located at the position normally occupied by the globar source in a Perkin-Elmer infrared spectrometer.(10) This point is conjugate with the entrance slit of the spectrometer, and therefore the surface of the sample at A is effectively imaged on the entrance slit. The spectrometer was operated in the normal manner and the spectra obtained as tracings from a Leeds & Northrup strip-chart recorder.

The samples were sections cut from two types of turbine blades, and a specimen of boride composition material. Chromel-alumel thermocouples were welded to the turbine blade samples; the refractory boride material could not be welded, so in this case the thermocouple was jammed between two pieces of the material, which were then cemented together with refractory cement. Some of the samples used are shown in Fig. 23.

For comparison purposes a number of sources of blackbody radiation were used. These included a globar radiator, wedge-shaped pieces of oxidized iron, and a cavity radiator of oxidized steel.

---

(10) Barnes, McDonald, Williams, and Kinnaird, J. App. Phys. 16, 77 (1945).

The globar is a standard commercial radiation source of known emissivity.[11] The wedges were set with their openings facing toward the spectrometer; since the emissivity of iron oxide is above 0.95 [12] such a wedge is effectively a blackbody radiator. The cavity radiator consists of two pieces of steel bolted together, with a wedge-shaped slot cut out at one end. The source of radiation is the interior of the wedge-shaped cavity and this is effectively a blackbody. The heat capacity of this construction is relatively large, so that its temperature could be precisely controlled.

The spectrum was scanned from 1 to 3 microns at various temperatures in the range 1000° to 2000° F. A typical example of the emission spectra obtained in these measurements is given in Fig. 24. As usual with solid radiators, the spectra have the general appearance of the emission from a blackbody, modified by atmospheric absorption. The relative emissivity of a given sample at any wavelength is equal to the ratio of its measured intensity of emission at that wavelength to the intensity of emission from a comparison standard at the same temperature.

Referring to Fig. 24, if we let $I_o(\lambda)$ stand for intensities on the upper (blackbody) curve, and if $I(\lambda)$ represents intensities on the lower (specimen) curve, then the emissivity of the specimen at any wavelength λ is given by

$$e_\lambda = I(\lambda)/I_o(\lambda).$$

Then to obtain values of e_λ over the spectrum, $I(\lambda)$ and $I_o(\lambda)$ must be measured and a computation carried out for each value of λ. However, in this work our primary interest was to obtain experimental values of the ratio $(J_{\lambda_1}/J_{\lambda_2})$ for various choices of λ_1 and λ_2, and to observe how closely these could be correlated with the theoretical curves, on the assumption that the spectral emissivities are equal at the two wavelengths.

Therefore, instead of following the tedious procedure of point-by-point measurement of emissivities, a direct method was used. This consisted of plotting values of the ratio $J_{\lambda_1}/J_{\lambda_2}$ against temperature, for various choices of λ_1 and λ_2. The values of J_{λ_1}, and J_{λ_2} were read directly from the measured spectra. The resultant plots were compared to theoretical plots calculated for the

(11) S. Silverman, J. Opt. Soc.Am. 38, 939 (1948).
(12) "Temperature" (Reinhold, New York, 1941) p.1313.

same pairs of wavelengths.

A typical comparison of theoretical and experimental curves is shown in Fig. 25, where the experimental plot has been normalized with respect to slitwidth. Close agreement between the theoretical and experimental curves is evident. Precise agreement at every point is unimportant because of the relative nature of the calibration; what is important is that the slopes of the theoretical and experimental curves should be equal at every temperature. When this is the case, one knows that the measured ratio is strictly a function of temperature, and independent of such extraneous quantities as surface emissivity, atmospheric absorption, and combustion gas radiation.

For the wavelengths 1.67μ and 2.10μ of Fig. 25 the bandwidths are 0.011μ and 0.0095μ respectively; the ratio $\Delta\lambda_2/\Delta\lambda_1$ of equation (II.5) is equal to 0.011/0.0095 = 1.16, and we can write

$$J_{1.67}/J_{2.10} = 1.16\ (I_{1.67}/I_{2.10}) \qquad \text{(III.1)}$$

The solid curve in Fig. 25 is a plot of the ratio $I_{1.67}/I_{2.10}$ against temperature, as measured by the infrared spectrophotometer, while the dotted curve is a plot of $J_{1.67}/J_{2.10}$, calculated from equation (9). The small crosses are values calculated by multiplying the points on the solid curve by the factor 1.16, as required by equation (III.1). The curve determined by the crosses coincides with the theoretical curve within the precision of measurement. Plots of this type were obtained for each of the samples and these experimental curves bear out equation (II.4) with a high degree of accuracy. This indicates that the assumption $e_{\lambda_1} = e_{\lambda_2}$ is well founded. The emissivities of the samples varied by several percent dependent upon time and previous treatment of the specimen, although the ratios were always the same for a given temperature.

APPENDIX IV. DISPERSION OF FUSED QUARTZ IN THE INFRARED.

Measurements of quartz refractive indices in the near infrared were made by Müller and Wetthauer.[13] These measurements, extending as far as 2.6 microns, are given in Table IV. These refractive index data were fitted to a Hartmann formula with three constants,

$$n = A + \frac{B}{\lambda - \lambda_0} \quad , \qquad \text{(IV.1)}$$

where the constants in this equation are

$$A = 1.510 \ ,$$
$$B = 0.353 \ ,$$
$$\lambda_0 = 6.911\mu \ .$$

The bandwidth passed by the instrument was calculated from the data of Fig. 26. The dispersion was obtained by differentiating equation (IV.1). This gives

$$\frac{dn}{d\lambda} = -B/(\lambda - \lambda_0)^2 \ . \qquad \text{(IV.2)}$$

The bandwidth was calculated as the sum of the Rayleigh term and a term due to finite slits. The Rayleigh term is given by

$$\Delta\lambda = \lambda/S \ (dn/d\lambda) \qquad \text{(IV.3)}$$

Where S is the prism base.

(13) C. Müller and A. Wetthauer, Z.f. Physik 85, 559 (1933)

The finite slit term was calculated assuming minimum deviation for both wavelengths. The usual approximate formula for a Littrow spectrometer was used. This formula is obtained as follows. Consider a Littrow prism monochromator. The linear distance along the spectrum at the exit slit is $f\Delta\lambda(d\theta/d\lambda)$, where f is the focal length of the collimator, and $d\theta/d\lambda$ is the angular dispersion. If $\Delta\lambda$ is now the interval covered by a single slit image, then

$$S_2 = f\Delta\lambda(d\theta/d\lambda) \qquad \text{(IV.4)}$$

is the width of the image. Since entrance and exit slits are normally equal, the width of the entrance slit image is also

$$S_1' = f\Delta\lambda(d\theta/d\lambda) \qquad \text{(IV.5)}$$

The bandwidth passed by the exit slit is then

$$\Delta\lambda = \frac{S_1 + S_2}{2f(d\theta/d\lambda)} \qquad \text{(IV.6)}$$

The factor of 2 occurs due to the fact that the prism is traversed twice.

At minimum deviation the index of refraction is given by

$$n = \sin\tfrac{1}{2}(\alpha+\theta)/\sin\tfrac{1}{2}\alpha\,, \qquad \text{(IV.7)}$$

where α is the prism angle; we then have

$$\frac{d\theta}{d\lambda} = (d\theta/dn)(dn/d\lambda) \qquad \text{(IV.8)}$$
$$= \frac{2}{n}\tan\tfrac{1}{2}(\alpha+\theta)\frac{dn}{d\lambda}\,.$$

Substituting equations (IV.7) and (IV.8) into equation (IV.6) we get

$$\Delta\lambda = \frac{(1 - n^2 \sin^2 \tfrac{1}{2}\alpha)^{1/2}}{4 \sin \tfrac{1}{2}\alpha \, (dn/d\lambda)} \quad \frac{S_1 + S_2}{f} \qquad \text{(IV.9)}$$

where $(dn/d\lambda)$ is given by IV.2. The calculated bandwidth is plotted in Fig. 27, which shows the Rayleigh and finite slit terms separately.

APPENDIX V. TEMPERATURE COEFFICIENTS OF LEAD SULFIDE PHOTOCONDUCTIVE CELLS.

The use of lead sulfide photoconductive cells in infrared measurements has become widespread in recent years. The lead sulfide cell is superior to the older heat detectors for work in the region 1-3 microns. The sensitivity of lead sulfide cells in this region is greater than that of the heat detectors by several orders of magnitude, and the signal-to-noise ratios obtainable in practice are also superior. In addition, the lead sulfide cell is capable of greater speed of response than any heat detector.

For precise photometric measurements lead sulfide cells have the drawback that they have large temperature coefficients of sensitivity. An instrument using a lead sulfide cell for measurement of radiant intensity must therefore be carefully thermostated or compensated, and calibration for photometric measurements must be made for a specific cell temperature.

In a ratio instrument, such as the DICHROMATIC RADIATION PYROMETER, the temperature coefficient of sensitivity affects the intensity measurements at both wavelengths used in the instrument. Therefore, providing only that the temperature coefficient is the same at both wavelengths, the effect of temperature of the cell should be cancelled out and should not affect the operation of the instrument. It is also necessary, incidentally, that the frequency response be the same at both wavelengths, but this is well

known to be the case.[14]

It is known from previous measurements [15] that some types of evaporated lead sulfide cells show a spectral differential with respect to temperature coefficients of sensitivity. A lead sulfide cell having such characteristics would be disadvantageous for a ratio instrument, since the desired cancellation of the temperature effect would not be obtained.

Chemically deposited lead sulfide cells of high quality have recently become available from the Eastman Kodak Company. These cells show marked superiority over previous evaporated-type cells with respect to sensitivity, signal-to-noise ratio, and uniformity. Measurements were made to verify the temperature coefficient of sensitivity of several Eastman Kodak lead sulfide cells at different wavelengths. Examples of the results of these measurements are shown in Fig. 28 and in Table V. Over the range of wavelength 1-3 microns, the temperature coefficient of sensitivity was found to be constant for ambient temperatures ranging from 60° to 95° F. It therefore appears that these cells are suitable for all ordinary applications of a ratio instrument, and that the temperature change of cell sensitivity can be assumed to cancel.

APPENDIX VI. ANALYSIS OF SEVERAL METHODS OF SEPARATING WAVELENGTHS.

Having selected the detector and chosen the principle of using a single detector, it was next necessary to consider the method of separating the two wavelengths in the optical system. One method, which has been used successfully in instruments for the visible region, is to provide the monochromator with two exit slits at different positions in the focal plane of the spectrum. In the present case, however, the separation of the two wavelengths and the dispersion were such that the linear separation in the exit slit plane would have been inconveniently small. In addition, it was desired to construct the instrument in such a way that the two wavelengths could be varied over a considerable range subsequent to

(14) Mroszowski, McMichael, and Knetko, Bull.Am.Phys.Soc. 28, 36 (1953)

(15) Tourin, Hecht, Tandler, and Grossman, Industrial Scientific Co. report 225-1 (1952), on Air Force contract W33(038)-10514.

completion of construction of the instrument, and the use of a two-slit system would have required a mechanical arrangement to enable moving the slits with respect to one another, with attendant difficulties of optical alignment. Also, an optical system would have had to be provided to recombine the two separated beams onto a single detector. For these reasons it was considered preferable to make this first model with a single exit slit.

Since it was desired to use AC amplification of the electric signal, modulation of the light beam was necessary. Because of this fact and the desirability of using a single slit, the possibility was considered of operating the instrument by oscillating the Littrow mirror on the monochromator. This has been done successfully for scanning purposes.[16,17] In this scheme the oscillation of the Littrow mirror serves both to separate the wavelengths and to modulate the light beam, so that no chopper is necessary. In addition, in this system the full aperture of the instrument is used for both wavelengths. On the other hand, upon analysis the mechanical problems involved in providing such an oscillating mirror system and insuring a high degree of stability appeared to be excessive.

Finally, another method of separating the two wavelengths is to split the spectrometer optical system in half in a horizontal plane, using one-half of the instrument for each wavelength. In the Littrow-type instrument the wavelength transmitted by the exit slit is governed by the angular position of the Littrow mirror. Therefore, if the Littrow mirror is split in a horizontal plane, each of the two halves independently determines a given wavelength transmitted at the exit slit. The Littrow mirror is an aperture stop: every point on the entrance slit contributes to the illumination of the entire mirror, and likewise the entire mirror contributes to every point on the exit slit. Therefore, each half of the split mirror illuminates the entire exit slit and two independent spectra occur which overlap at all points in the vertical direction.

Separation of the two wavelengths at the detector is most simply accomplished by synchronous modulation of the light beams. This is done by means of a chopper, or sector disc, cut in such a way as to interrupt the two beams at different times. The question then remains as to where this chopper can be most effectively located. In an instrument of the analytical type where the source of radiation is at a fixed location, a suitable spot for the sector disc is at a point conjugate to the Littrow mirror.[18] In this method the two halves of the Littrow mirror are effectively modulated separately,

---

(16) B.W.Bullock and S.Silverman, J. Opt.Soc.Am.40, 608 (1950).
(17) Wheatley, Vincent, Rotenberg, and Cowan, J.Opt. Soc.Am. 41. 665 (1951).
(18) A.Savitzky and J.C.Atwood, Symposium OSU June 1952,Paper #16

so that the two spectra can be superimposed at the exit slit. This has the two-fold advantage of permitting use of the full slit for both wavelengths and introducing no complications into the optical alignment, since the system is simultaneously aligned for both beams. On the other hand, the DICHROMATIC PYROMETER was designed for sighting on a target source of radiation which is not in itself part of the instrument, nor is the source necessarily at a fixed distance. The conjugate point to the Littrow mirror is therefore not always near a focal plane, so that an inconveniently large sector disc would have been required to avoid obstructing the light beam. For these reasons it was decided to make a slight sacrifice in energy and ease of alignment, and to separate the beams at the entrance and exit slits.

In the method employed the two spectra do not completely overlap at the exit slit, but are displaced vertically from one another approximately half the width of the slit. The chopper disc is located close to the plane of the entrance slit. Each half of the slit thereby contributes to only one of the two wavelengths. The energy in each is thereby reduced by half; because abundant energy is available this loss is of no importance. The displacement of the two spectra at the exit slit is obtained by slightly tilting the two halves of the Littrow mirror away from the vertical so that one of the spectra at the exit slit is shifted upward and the other downward.

APPENDIX VII. ENERGY IN THE DICHROMATIC PYROMETER.

The total power received by the photocell is given approximately by

$$E'_{total} = \pi B_\lambda \sin^2\theta' \alpha_\lambda A_D \Delta\lambda \ , \qquad \text{(VII.1)}$$

where B_λ is the spectral brightness of the source, given by

$$B_\lambda = c_1 \lambda^{-5} (\epsilon^{c_2/\lambda T} - 1)^{-1} \ , \qquad \text{(VII.2)}$$

α_λ is the transmissivity of the optical system, and equals about 0.5, A_D is the effective area of the detector,

$$A_D = \frac{1}{6} \text{ (slit height x slit width)}, \qquad \text{(VII.3)}$$

$\Delta\lambda$ is the bandwidth, and is proportional to the slit width (see equation (IV.9)), and θ' is the angle subtended at the detector by the exit pupil of the optical system.

Equation (VII.1) is obtained as follows:

The quantity $\pi B \sin^2\theta'$ gives the geometrical illumination (energy per unit time per unit area) on the detector; the proof may be found in any text on geometrical optics.* In this expression B is the brightness of the source of radiation. The detector in the DICHROMATIC PYROMETER is illuminated by monochromatic radiation of spectral brightness B_λ and bandwidth $\Delta\lambda$; hence the source brightness is $B_\lambda \Delta\lambda$. The geometrical illumination is reduced by reflection and other losses in the optical system, which accounts for the factor α_λ. Lastly, the <u>total</u> energy received by the detector equals the illumination times the illuminated area A_D, and this is governed by the slit width setting. The factor of $\frac{1}{6}$ occurs due to image reduction in the optical system.

* e.g. Hardy and Perrin, The Principles of Optics (McGraw Hill Book Co., New York, 1932).

APPENDIX VIII. SELECTION OF WAVELENGTHS.

We sought a combination of wavelengths which would give an intensity ratio approximately equal to unity at one end of the temperature scale, decreasing towards the other end. In addition, for sufficient sensitivity we required the ratio change between 1000° and 2000° F. to be between 2 and 3. To avoid the region of atmospheric absorption, we could select wavelengths in the following bands:

1.40 μ to 1.79 μ

1.99 μ to 2.12 μ

2.35 μ to 2.51 μ.

The peak wavelengths are given by

$$\lambda_m T = 0.2834 \text{ cm-deg}$$

This gives us 3.57 μ for 1000° F and 2.12 μ at 2000° F. the peak wavelength at 1000° F is beyond the long wavelength limit of quartz transmission. Therefore, it is impossible to obtain a ratio of unity at the low temperature end of the scale, since this requires straddling the peak. Therefore the reciprocal ratios were chosen, to obtain unity ratio near the high end of the scale. The ratios, and temperature change with ratio are given in Table VI for various wavelengths.

APPENDIX IX. THE DETAILED CIRCUIT DIAGRAMS

1. The Pre-Amplifier

The pre-amplifier circuit is shown in Fig. 29. It employs a miniature twin-triode type 12AX7. One of the triodes serves as a cathode follower output tube. The PbS cell is biased by way of a 20 meg resistor. The input signal to the pre-amplifier is developed across this 20 meg resistor. All components shown inside the dashed rectangle are contained in a convenient plug-in unit.

2. The Amplifier

The amplifier circuit is shown in Fig. 30. Tube V_1 is a type 6SN7 and represents an additional cathode follower. Although it is not essential to the operation of the circuit at present, it was incorporated in order to make feasible the insertion of an automatic volume-control by means of a low-resistance servo-potentiometer connected across the output of this cathode follower. Tube V_2 is a type 6SL7 twin-triode connected in a two-stage resistance-coupled amplifier. The output of the second stage of V_2 is fed into the signal grid of V_3, which is a type 6SN7. V_3 is operated as a cathode follower. Part of the output of V_3 is fed back to the cathode of the first stage of V_2. This produces overall negative feedback across the amplifier and linearizes and stabilizes its response. The output of V_3 is fed into a differentiating network represented by the condenser C and the resistor R. Fig. 31a shows the typical form of the signal at the output of the cathode follower V_3 and Fig. 31b shows the signals produced across the resistance R. The amplitudes of the unidirectional peaks of the differentiated pulses are proportional to the amplitudes of the rectangular pulses.

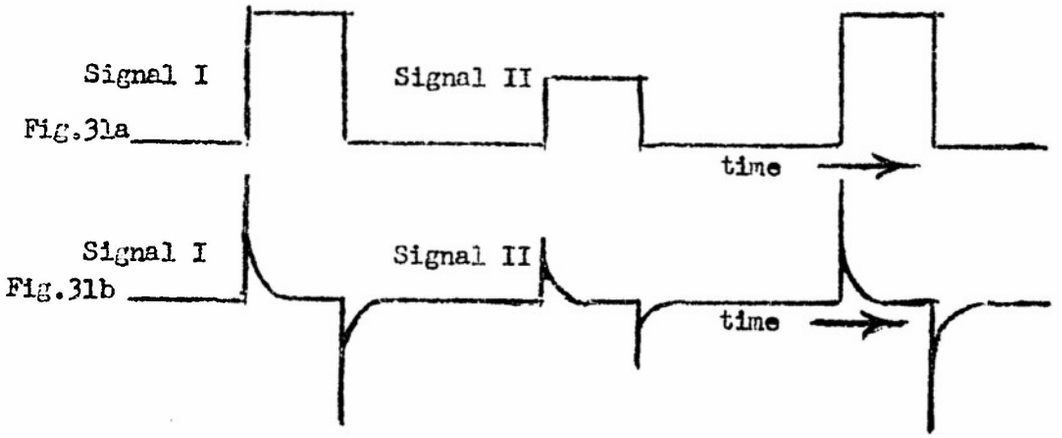

Fig.31a

Fig.31b

Signal I corresponds to wavelength λ_1 and Signal II corresponds to wavelength λ_2. The duration of the pulses after differentiation is much shorter than before. The time separation between the pulses of equal polarity of signals I and II after differentiation is therefore much longer than at the output of V_3. This latter fact is very advantageous in view of the necessity of achieving a clean separation of signals I and II into rectifiers I and II. This is due to the fact that slight errors in the synchronism of the synchronous commutator might cause mixing of the signals in rectifiers I and II if the time separation between signals I and II were too short. Even though phase-shifts in the amplifier should have a negligible effect, there is an additional possibility of error represented by the fact that the rise time and decay time of the original pulses will be somewhat lengthened by the amplifier. The differentiation will have a useful effect also because of that.

The signal across resistor R is led to the synchronous commutator, which is synchrononized with the radiation chopper, and which feeds signal I only into the upper half of V_4 and signal II only into the lower half of V_4. V_4 is a vacuum tube twin-diode type 6H6 of which each half detects only the positive pulses indicated in Fig. 31b. The outputs of rectifiers I and II are led directly to the ratio circuit.

3. The Ratio Circuit

Fig. 32 shows the ratio circuit. The balanced vacuum tube voltmeters I and II are represented by tubes V_5 and V_6 which are twin-triodes type 5691.

One half of V_5 serves as signal tube and the other half as balancing tube and likewise for V_6. The outputs are derived across the cathodes of V_5 and V_6. The current meters M_I and M_{II}, which are connected across these outputs by way of fixed resistors, are microammeters of 200μa full scale. The deflection of each meter is proportional to the signal in its channel.

Tubes V_5 and V_6 can be balanced by individual potentiometers to which their cathode resistors are connected. The slides of these pots are connected to ground. These pots serve as zero adjusters for the meters M_I and M_{II}. The balanced output of V_6 is connected to the input of the servo-amplifier in series with a resistor and potentiometer circuit.

The servo-amplifier is a Brown type 351921. The servo-motor is also made by Brown Instrument Division. Its speed is 27 RPM. The servo-amplifier and motor constitute a combination indicator

and recorder system. The self-balancing potentiometer R_p is wire-wound and has a resistance of 10KΩ. It is a multi-turn Helipot product.

4. Analysis Of The Ratio Circuits

Fig. 33 indicates the method in detail. E_2 is the output of the balanced tube-voltmeter II. E_o is the potential of a dry cell. The servo-motor adjusts the slide of R_p so that no current flows through the input terminals of the servo-amplifier. For servo system balance therefore:

$$E = E_2 \qquad \text{(IX.1)}$$

For the balanced system, Kirchhoff's Laws give consequently:

$$E = E_o \frac{R_R + R_{c_1}}{R_c + R_p + R_s} \qquad \text{(IX.2)}$$

Equations (IX.1)and (X.2) give:

$$R_{p_1} = \frac{E_1}{E_o} - \frac{E_2}{E_1}(R_c + R_p + R_s) - R_{c_1} \qquad \text{(IX.3)}$$

If one adjusts the common volume control to keep E_1 constant, the position of the self-balancing potentiometer is a function of E_2/E_1 or I_2/I_1. Using the same definitions as above, equation (IX.3) gives the following values for $R_c + R_s$ and R_{c1}:

$$R_c + R_s = R_p \left(\frac{E_o}{E_{2\,max} - E_{2\,min}} - 1 \right) \qquad \text{(IX.4)}$$

$$R_{a_1} = R_p \left(\frac{E_{2min}}{E_{2max.} - E_{2min}} \right) . \qquad (IX.5)$$

Where E_2 max and E_2 min are the signals corresponding to the upper and lower ends of the temperature scale.

APPENDIX X. CALIBRATION OF THERMOCOUPLES.

For measurement of temperatures of turbine blade samples, a chromel-alumel thermocouple and potentiometer-indicator were calibrated by the Pyrometry Section, National Bureau of Standards, for the range 32°-1530° F. Twenty working thermocouples were then calibrated against the standard in our laboratory. The NBS calibration is given in Table VII.

Curves were first plotted for the NBS calibrated thermocouple and potentiometer: (1) temperature vs. scale, (2) emf vs. scale, and (3) emf vs. temperature. An example is shown in Fig. 34. The emf vs. temperature curves were extrapolated to 2000° F.

A cubic equation of the type

$$emf = a+bt+ct^2+dt^3$$

with t as the temperature and a, b, c, and d as constants, was derived. Although the Emf vs. Temperature curve is practically straight, a quadratic equation did not produce as good a fit with the calibration data as did the cubic equation.

A voltage divider was used in order to extend the potentiometer range for temperatures up to 2000°. It consists of two 1000 ohm resistors soldered together, the potentiometer being connected across one resistor and the thermocouple connected across both. The circuit arrangement is shown in Fig. 35. The values of

resistance were chosen large, in order to minimize the current in the thermocouple. This voltage divider was used for most of the calibration. However, with these resistors the potentiometer was hard to read: a change of 20 scale divisions produced a corresponding deflection of the galvanometer of less than one division and, when the potentiometer was balanced, the scale could be changed by two divisions either way before the meter moved visibly, corresponding to an emf change of 0.13 millivolts or to a temperature change of roughly 5°F.

In order to increase sensitivity, the voltage divider was changed to one consisting of two 47 ohm resistors. In general, the readings were more precise than those taken with the 1000 ohm voltage divider. Temperatures measured on the NBS calibrated thermocouple with this voltage divider agreed very well with the temperatures measured without a voltage divider (below 1500°F). While the working thermocouple reading was less than that of the NBS calibrated thermocouple by only three scale divisions at most, as measured with the 1000 ohm divider, the reading of the working thermocouple with the 47 ohm voltage divider was 15 scale divisions less than the NBS calibrated thermocouple at high temperatures and 8 scale divisions less at low temperatures. Therefore, current may flow through the thermocouple circuit, and at high temperatures, the 47 ohm voltage divider may not be as accurate as the 1000 ohm divider.

The method of taking measurements was as follows: The working thermocouple and NBS calibrated thermocouple were twisted together with their junctions in contact. The two thermocouples were admitted into the furnace and the temperature was adjusted for approximately 50° intervals between 1000° and 1950° F. Readings of both thermocouples were taken as quickly as possible, along with the room temperature, as read at the check coil of the potentiometer, when the furnace had come to equilibrium. Readings were made by setting the potentiometer for a scale reading a little too high with the galvanometer needle just discernibly off center, then setting the potentiometer for a scale reading a little too low with the needle again off center, and finally taking the mean of the scale readings.

In order to find the emf developed at its terminals by a thermocouple, it was necessary to compare the thermocouple readings with and without the voltage divider. A run was made between 1000° and 1530° with the NBS calibrated thermocouple. Readings were taken with and without the voltage divider. The emf was read off from the Emf vs. Scale curve. By dividing the "emf without the voltage divider" by the "emf with voltage divider" at the various temperatures and then calculating the mean of the quotients, the factor

by which the voltage as read with the voltage divider must be multiplied to get the voltage as produced by the thermocouple was computed. This dividing factor had a value of 2.001 for the 1000 ohm voltage divider and 2.026 for the 47 ohm voltage divider.

During the calibration, the reference junctions of the thermocouples were at room temperature. Since the room temperature fluctuated, corrections had to be made in order to have the reference junction temperature constant at 32°. For this purpose a thermocouple junction was immersed in an ice-water mixture, with its terminals left at room temperature. The thermocouple was calibrated against the emf for different room temperatures in the temperature range 73°-87°F. The emf was read off against the scale reading from the Emf vs. Scale curve and a room temperature vs. emf curve was plotted. This thermocouple was then used in the succeeding measurements as a reference junction.

The corrections that were made to obtain the temperature of the junctions are as follows: After the readings were taken, the voltage across the potentiometer was read off from the Emf vs. Scale curve for the scale reading of the NBS calibrated thermocouple. This voltage was multiplied by the voltage divider factor. To the product was added the voltage read off from the Emf vs. Temperature curve, in order to correct the reference junction from room temperature to 32°F. This gave the emf developed by the NBS calibrated thermocouple. Against this emf the temperature of the thermocouple junctions was read off from the emf vs. Temperature curve.

The corresponding correction for the scale reading of the working thermocouple undergoing the calibration run was obtained by first finding the voltage corresponding to the room temperature from the Room Temperature vs. emf curve for the thermocouple to be kept at the ice point. Since the emf vs. Scale curve is practically linear between 1000°-1950°F the slope is constant and equal to 32 scale divisions per millivolt. The scale correction was obtained by multiplying the voltage corresponding to the difference between room temperature and 32°F. (the temperature of the reference junction) by 32 scale divisions per millivolt, and then dividing by the voltage dividing factor. This correction was added to the scale reading of the potentiometer when the reference junction was at room temperature, to get the scale reading with the reference junction at 32°.

The data and calculations are given in Table VIII. In the first column is the temperature to which the furnace was set. The second column contains the room temperature, as measured at the manganin

check coil of the potentiometer. The third and fourth column refer to the potentiometer scale reading of the thermocouples as read at the particular furnace temperature. The emf coinciding to the check-coil temperature (referred to 32°F) is listed in the fifth column as read from the emf vs. temperature curve of the NBS-calibrated thermocouple. In the sixth column is the voltage coinciding to the scale reading of the NBS-calibrated thermocouple, as read from the emf vs. scale curve. The seventh column contains the corrected emf of the NBS-calibrated thermocouple, the coinciding temperature appearing in the ninth column. The scale correction in the eighth column is to be added to the scale reading at the thermocouple undergoing the calibration (in accordance with the method described above). The corrected scale reading is in the tenth column. Finally, curves of temperature (ninth column) vs. potentiometer scale (tenth column) were plotted for the various working thermocouples. The calibration curves are very similar, differeing by no more than 50°F from each other for a given scale reading.

Temperatures indicated with the standard and working couples were checked at five points in the range 1000°-2000°F. An example of the results of this calibration has been given in Fig. 34.

TABLE I. FIRST COMPARISON OF DICHROMATIC PYROMETER AND THERMOCOUPLES.

Thermocouple Readings (°F)

Thermo-couple No.	16	15	14	13	Average	Reading between	Dichromatic Reading (Scale Div)
			1431	1421	1426	13 & 14	51
	1654	1620	1598	1590	1609	14 & 15	43
	1715	1688	1670	1658	1679	14 & 15	50
	1754	1726	1706	1700	1722	14 & 15	54
	1792	1766	1743	1735	1755	14 & 15	58
	1842	1815	1790	1782	1803	14 & 15	64.5 - 65
	1797	1766	1733	1720	1750	ditto	60
	1765	1736	1706	1695	1721	ditto	54.5
	1698	1675	1650	1640	1662	ditto	40
	1634	1614	1590	1581	1602	ditto	39
	1611	1592	1567	1560	1580	ditto	35.5
	1414	1397	1382	1380	1390	ditto	15.5
	1300	1290	1281	1281	1286		4
	12	11	10	9			
	1290	1298	not installed	1321		10 & 11	0-
	1349	1361	---	1389		ditto	6

TABLE II. EARLY MEASUREMENTS WITH DICHROMATIC PYROMETER

Thermocouples				
15	14	T	Mean	Dichromatic (Scale Div.)
157°F	1150°F	7	1153.5°F	37.0
1221	1212	9	1216.5	42.0
1254	1246	8	1250.0	47.0
1334	1321	13	1328	59.0
1374	1357	17	1365.5	67.0
1421	1405	16	1413	73.5
1467	1452	15	1459.5	82.0
1179	1169	10	1174	32.5
1239	1228	11	1233.5	45.0
1254	1246	8	1250	47.5
1312	1300	12	1306	59
1366	1351	15	1358.5	67.5
1429	1412	17	1420.5	75.5
1451	1435	16	1443	80
1488	1471	17	1479.5	87
1449	1431	18	1439	78
1428	1410	18	1419	72
1359	1346	13	1352.5	67
1342	1325	17	1333.5	64
1256	1245	11	1250.5	43.5
1215	1207	8	1211	38
1186	1181	5	1183.5	34.5

TABLE III. FINAL MEASUREMENTS WITH DICHROMATIC PYROMETER

Thermocouples				Dichromatic
13	14	15	16	Rec. Div.
1359°F	1365°F	1385°F	1436	29.2
1351	1357	1374	1427	27.5
1364	1371	1387	1442	27.5
1359	1366	1379	1430	29
1366	1372	1389	1445	27.0
1369	1372	1390	1447	29.5
1371	1382	1398	1450	28.5
1484	1492	1505	1575	45.5
1485	1495	1510	1582	44.5
1569	1576	1591	1675	58.5
1593	1600	1614	1709	60
1477	1485	1502	1590	44
1367	1373	1392	1450	30
1283	1294	1310	1360	21.5
1378	1384	1400	----	27
1450	1455	1470		32.5
1521	1527	1540		42.5
1574	1584	1598		49.5
1506	1515	1527		42.
1471	1477	1493		38
1420	1426	1441		32
1376	1382	1398		26
1301	1304	1316		16.5

TABLE III. (cont.)

Thermocouples				Dichromatic Rec. Div.
13	14	15	16	
1220	1224	1233	----	7.5
1201	1205	1213		5.0
1186	1187	1198		3.5
1233	1236	1248		9
1264	1267	1278		12.5
1315	1320	1334		19
1352	1357	1370		23
1396	1402	1416		29
1448	1455	1470		35
1515	1522	1534		41
1592	1599	1613		50
1174	1180	1194		2.5
1246	1253	1266		10.5
1267	1274	1285		13
1283	1287	1302		15
1322	1331	1345		20
1372	1380	1393		28
1415	1424	1433		34.5
1464	1470	1483		41.5
1537	1546	1558		51.5
1610	1616	1633		63
1574	1581	1595		54
1446	1455	1470		39.5

TABLE III. (cont.)

Thermocouples			Dichromatic Rec. Div.
13	14	15	
1346	354	1368	27.5
1300	1306	1320	21.5
1184	1183	1200	7
1198	1205	1220	10
1305	1312	1326	22
1404	1411	1426	33
1498	1505	1522	44
1590	1598	1613	57
1491	1499	1515	44
1398	1406	1423	31
1286	1294	1309	17.5
1195	1200	1211	4
1202	1209	1225	10
1255	1263	1276	17.5
1337	1345	1360	28
1446	1455	1470	42
1549	1559	1574	52.5
1641	1650	1669	66
1143	1147	1159	2
1240	1247	1256	12.5
1352	1357	1370	25.5
1446	1453	1464	35
1539	1544	1556	46

TABLE III (concl.)

Thermocouples			Dichromatic Rec. Div.
13	14	15	
1650	1659	1673	58
1489	1495	1505	37.5
1400	1405	1416	27.5
1297	1302	1312	15
1203	1207	1217	6

TABLE IV. REFRACTIVE INDICES OF FUSED QUARTZ.

λ(μ)	n	λ(μ)	n
1.028	1.450	2.010	1.438
1.196	1.448	2.145	1.436
1.370	1.446	2.270	1.434
1.560	1.444	2.390	1.432
1.722	1.442	2.500	1.430
1.870	1.440	2.595	1.428

TABLE V. TEMPERATURE COEFFICIENTS OF LEAD SULFIDE CELLS

Spectrum Point	Intensity at 85°F	Intensity at 80°F	Ratio
1	3.25	3.63	1.12
2	4.40	4.81	1.09
3	5.30	5.85	1.10
4	5.95	6.62	1.11
5	6.59	7.28	1.11
6	7.12	7.90	1.11
7	7.27	8.09	1.11
8	7.02	7.85	1.12
9	5.75	6.45	1.12
10	4.56	5.14	1.13
11	3.91	4.38	1.12

TABLE VI. RATIOS AND TEMPERATURE VARIATION FOR VARIOUS CHOICES OF WAVELENGTHS

λ_1	R = 3 λ_1 Λ+1	R = 3.5 λ_1 Λ +1	R = 4 λ_1 Λ - 1	λ_2 (R = 3)	λ_2 (R = 3.5)	λ_2 (R = 4)
2.11	1.322	1.367	1.406	1.60	1.54	1.50
2.12	1.323	1.368	1.408	1.60	1.55	1.51
2.34	1.357	1.407	1.450	1.72	1.66	1.61
2.35	1.358	1.408	1.452	1.73	1.67	1.62
2.36	1.360	1.410	1.454	1.74	1.67	1.623
2.37	1.361	1.412	1.456	1.74	1.68	1.63
2.38	1.363	1.414	1.458	1.75	1.68	1.63
2.39	1.364	1.415	1.460	1.75	1.69	1.64
2.40	1.366	1.417	1.462	1.76	1.69	1.64
2.41	1.367	1.419	1.463	1.77	1.70	1.65
2.42	1.369	1.420	1.465	1.77	1.70	1.65
2.43	1.370	1.422	1.467	1.77	1.71	1.66
2.44	1.372	1.424	1.469	1.78	1.71	1.66
2.45	1.373	1.426	1.471	1.78	1.72	1.66
2.46	1.375	1.423	1.473	1.79	1.72	1.67
2.47	1.376	1.429	1.475	1.79	1.73	1.67
2.48	1.378	1.431	1.477		1.73	1.68
2.49	1.380	1.433	1.479		1.74	1.68
2.50	1.381	1.434	1.481		1.74	1.69
2.51	1.382	1.436	1.483		1.75	1.69

TABLE VII. CALIBRATION OF STANDARD THERMOCOUPLE AND POTENTIOMETER, AS CERTIFIED BY NATIONAL BUREAU OF STANDARDS TEST No.3.1d/129990

Lower Range Scale Reading	EMF Millivolts	Temperature °F	Upper Range Scale Reading	EMF Millivolts	Temperature °F
75.5	0.00	32	600	15.94	729
100	0.73	63	650	17.48	795
150	2.18	126	700	19.01	860
200	3.68	190	750	20.55	924
250	5.17	255	800	22.08	989
300	6.69	323	850	23.64	1054
350	8.22	392	900	25.18	1119
400	9.76	461	950	26.74	1185
450	11.31	529	1000	28.30	1252
500	12.85	596	1050	29.91	1320
550	14.39	663	1100	31.53	1389
600	15.93	729	1150	33.18	1460
			1200	34.83	1533

TABLE VIII. THERMOCOUPLE CALIBRATION DATA

CALIBRATION OF THERMOCOUPLE D

Furnace Temp.	Cold Junc.	Scale NBS	Scale D	Ecc.(NBS)	V(NBS)	E(NBS)	Scale Corr.	Temp.	Scale Read.
1000°F	76°F	420	419	1.03	10.39	21.82	16	977°F	435
1050	75	437	436	1.01	10.90	22.82	16	1020	452
1100	76	461	459	1.03	11.65	24.34	16	1084	475
1150	76.5	478	476	1.04	12.16	25.37	17	1127	493
1200	77	498	497	1.05	12.78	26.62	17	1180	514
1250	77	517	516	1.05	13.38	27.82	17	1232	533
1300	78	537	535	1.08	13.99	29.07	17	1285	553
1350	79	555	554	1.10	14.55	30.21	17	1332	571
1400	79	575	574	1.10	15.16	31.44	17	1385	591
1450	80	594	593	1.13	15.75	32.65	18	1437	611
1500	80	613	612	1.13	16.34	33.18	18	1487	630
1550	81	634	632	1.16	16.99	35.16	18	1546	650
1600	83	657	654	1.20	17.70	36.62	19	1610	673
1650	83.5	668	667	1.21	18.04	37.31	19	1641	686
1700	83	685	683	1.20	18.56	38.34	19	1686	702
1750	84	707	705	1.22	19.23	39.70	19	1746	724
1800	84	727	723	1.22	19.85	40.94	19	1802	742
1850	85	739	737	1.24	20.22	41.70	20	1835	757
1900	85	757	755	1.24	20.77	42.80	20	1886	775
1950	85	775	773	1.24	21.33	43.92	20	1938	793
1600	87	647	647	1.29	17.39	36.09	20	1587	667
1550	86	632	632	1.27	16.92	35.13	20	1544	652
1500	86	612	611	1.27	16.30	33.89	20	1886	631
1000	80	427	427	1.13	10.60	22.34	18	999	445

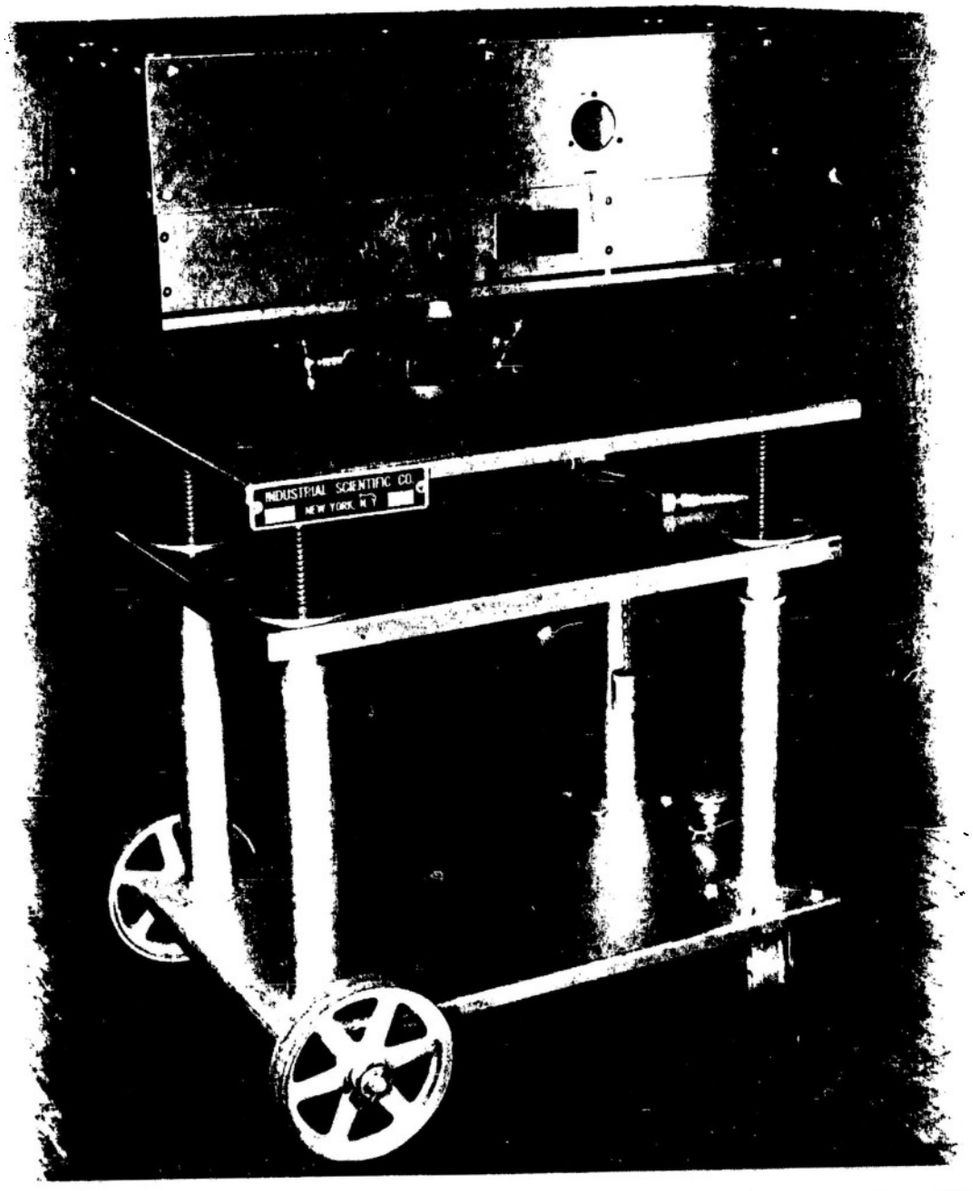

FIG 1 OPTICAL UNIT OF THE DICHROMATIC RADIATION PYROMETER.

FIG 2 ELECTRICAL SYSTEM OF THE DICHROMATIC RADIATION PYROMETER

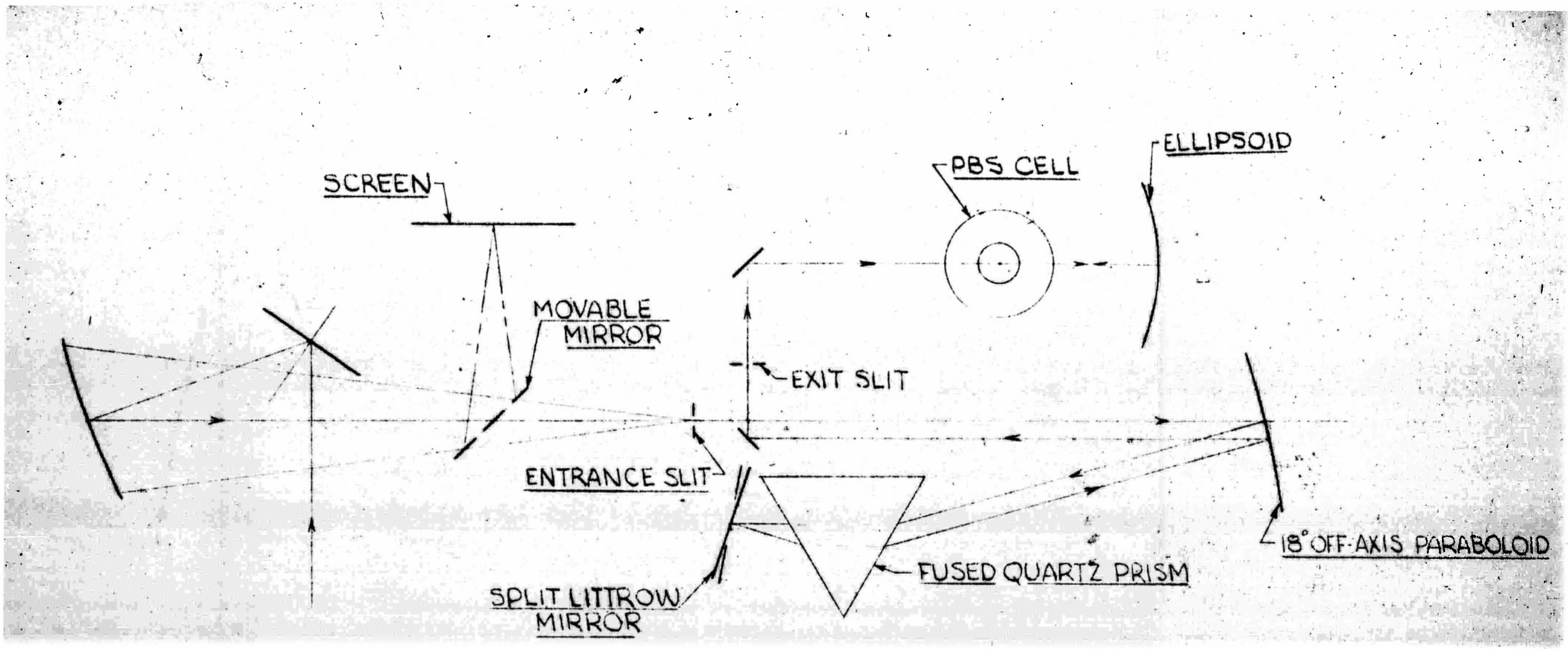

FIG. 3

No.	CHANGE	BY	DATE
4			
3			
2			
1			

9			
8			
7			
6			
5			

INDUSTRIAL SCIENTIFIC COMPANY
34 W. 33 ST.
NEW YORK 1, N. Y.

MACH. DICHROMATIC PYROMETER
ASS'Y.
PART SCHEMATIC OPTICAL LAYOUT

JOB 233
DR. AJF
DATE 1-4-54
CK.
DATE
SCALE
MAT'L
SIZE B2257

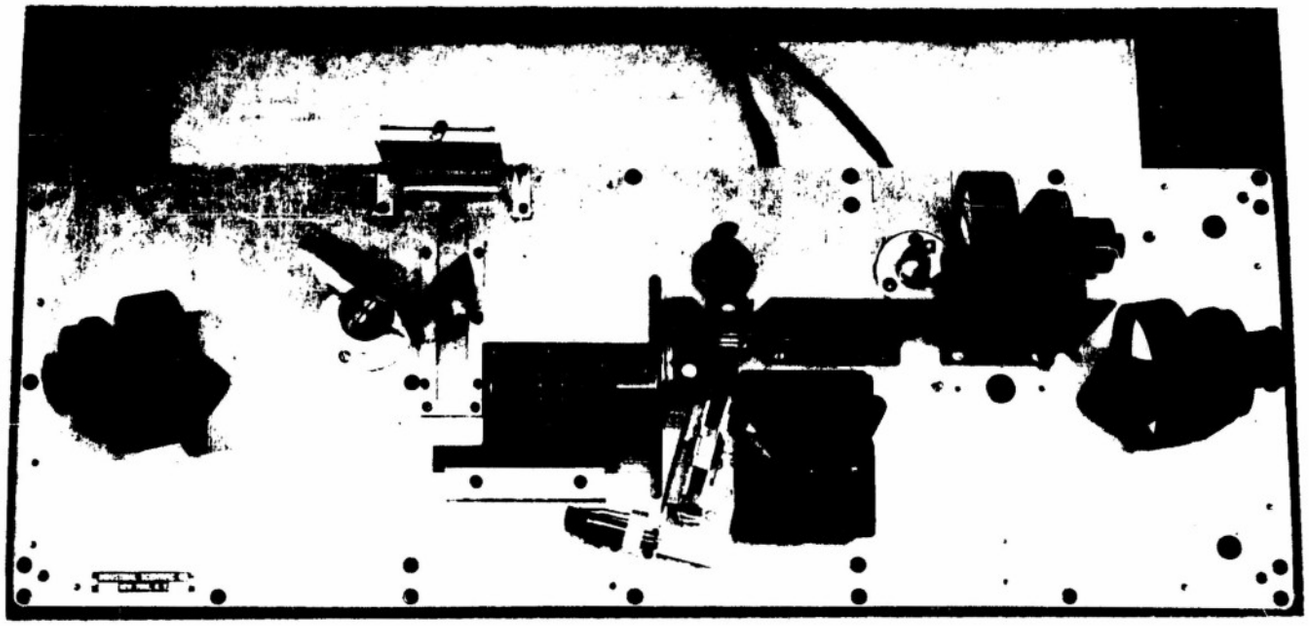

FIG. 4 TOP VIEW OF OPTICAL SYSTEM, DICHROMATIC RADIATION PYROMETER.

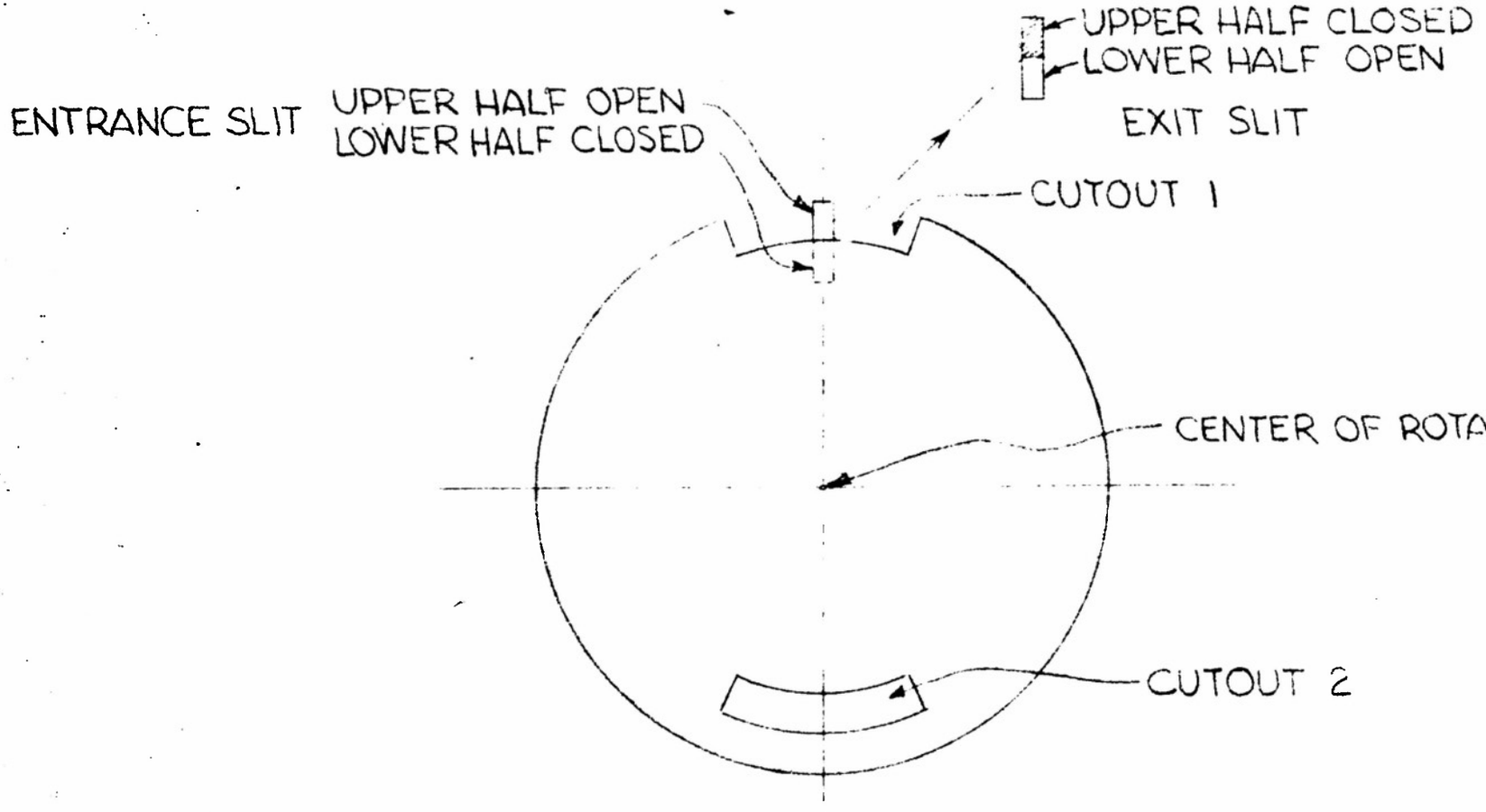

FIG. 5

No.	CHANGE	BY	DATE
4			
3			
2			
1			

9			
8			
7			
6			
5			

INDUSTRIAL SCIENTIFIC COMPANY
34 W. 33 ST.
NEW YORK 1, N. Y.

MACH. DICHROMATIC PYROMETER
ASS'Y.
PART CHOPPER DISC

JOB 233
DR. AJF
DATE 1-9-54
CK.
DATE
SCALE
MAT'L
SIZE A-5461

5

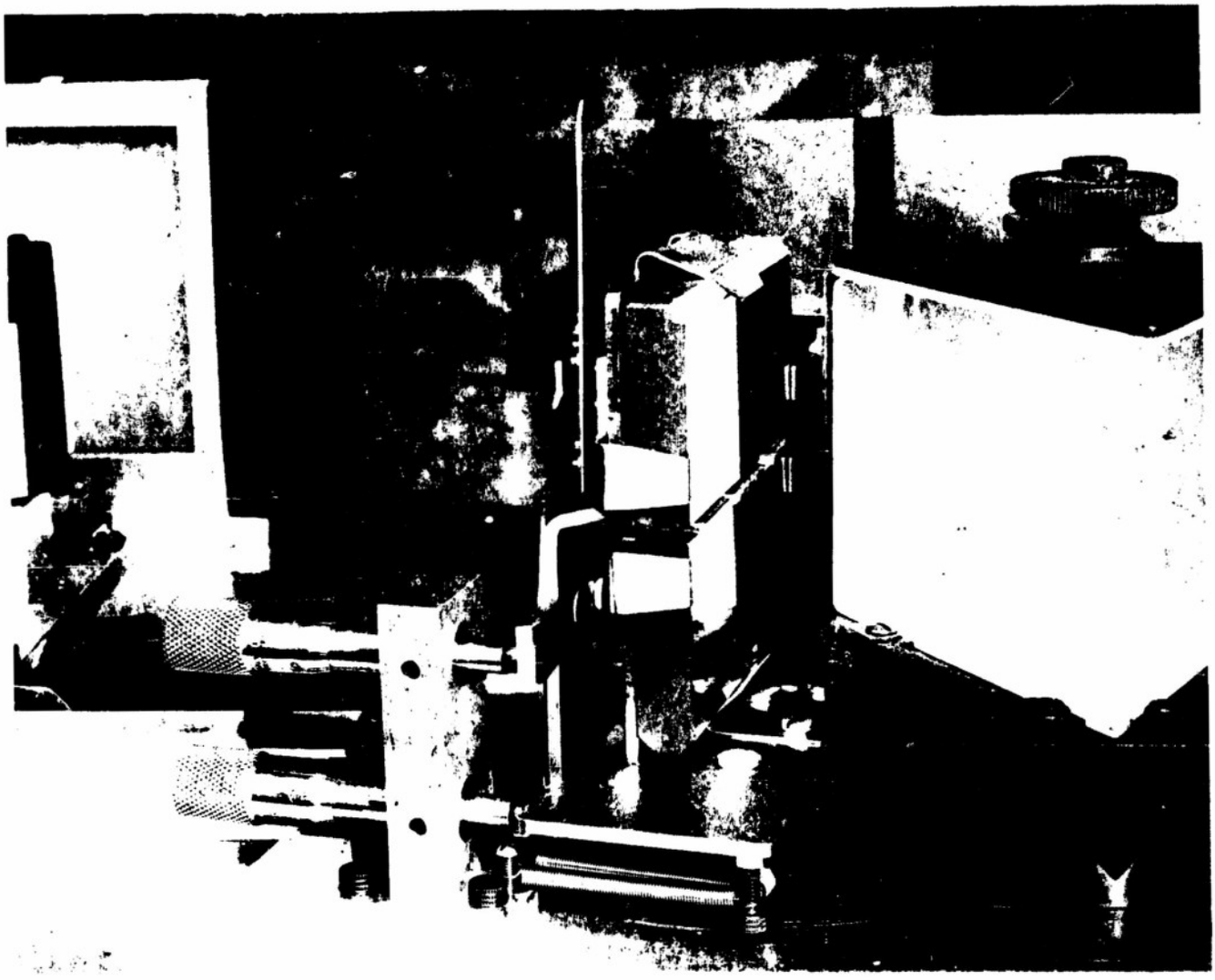

FIG. 6 SPLIT LITTROW MIRROR

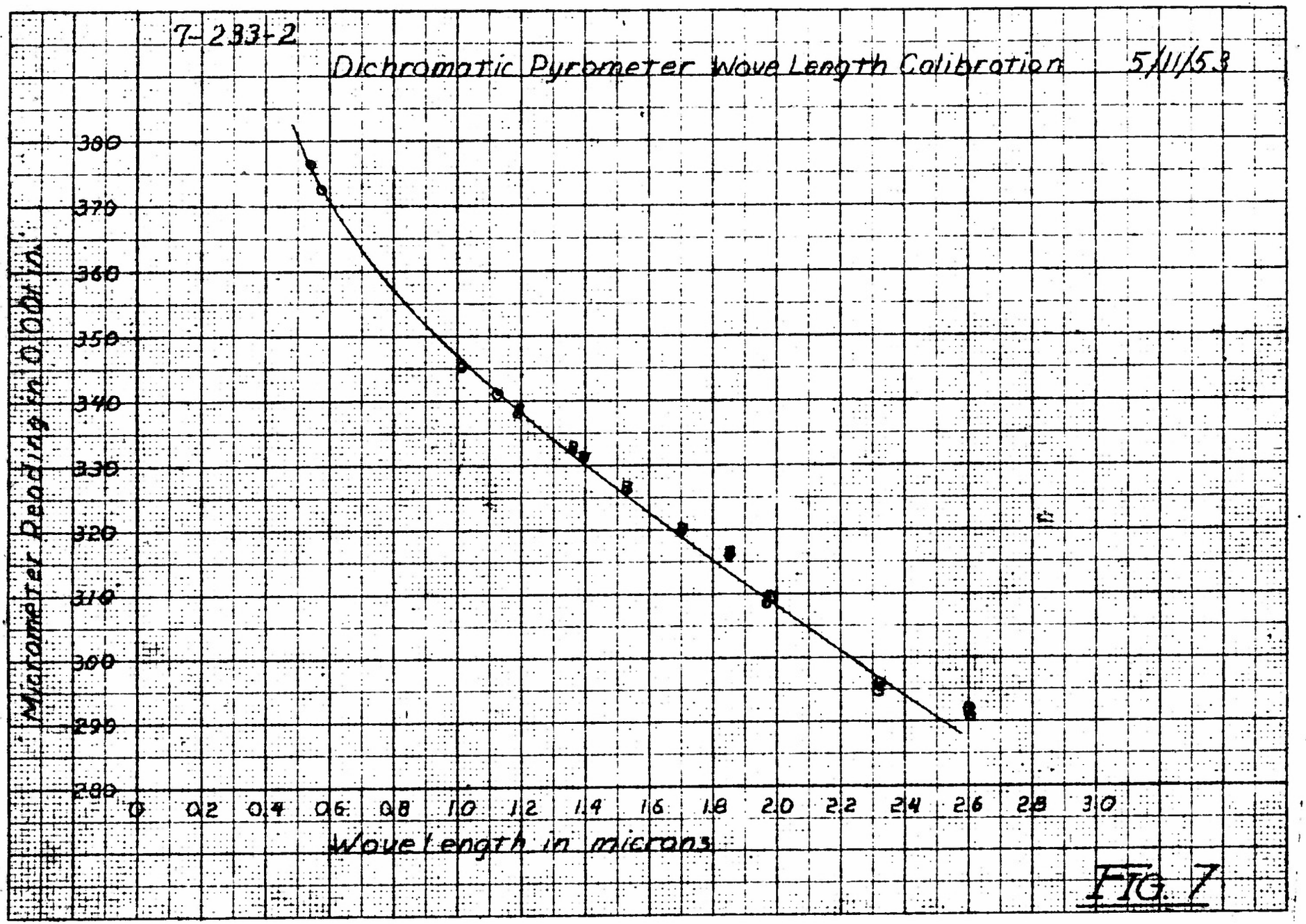

FIG. 7

ENTRANCE SLIT

(a)

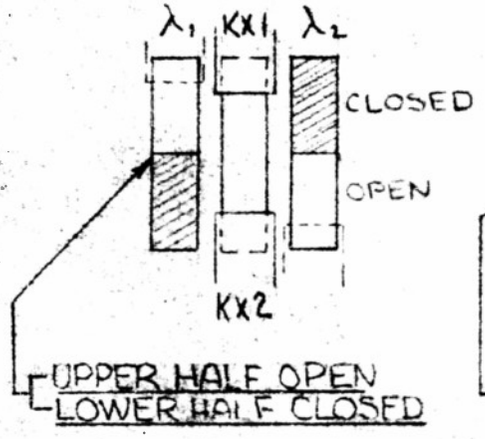

EXIT SLIT

(b)

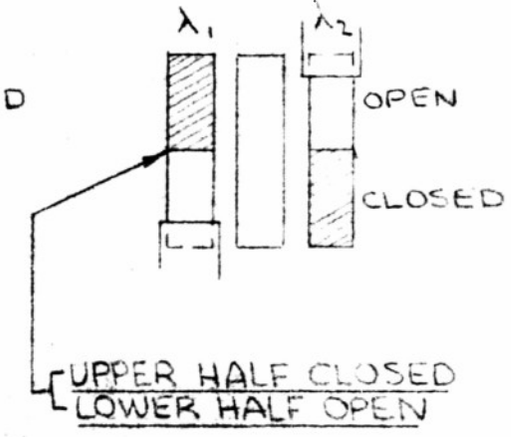

EXIT SLIT
FIRST POSITION

(c)

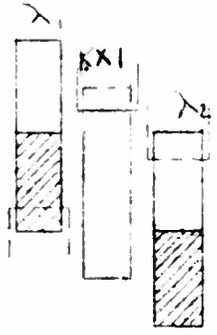

IMAGES DISPLACED
BY TILTING MIRRORS

EXIT SLIT
SECOND POSITION

(d)

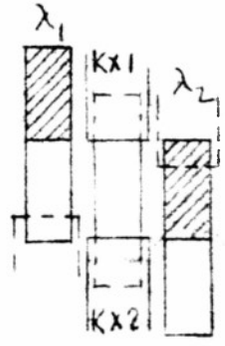

FIG. 8

No.	CHANGE	BY	DATE
4			
3			
2			
1			

9			
8			
7			
6			
5			

INDUSTRIAL SCIENTIFIC COMPANY
34 W. 33 ST.
NEW YORK 1, N. Y.

MACH. DICHROMATIC PYROMETER
ASS'Y.
PART SLIT IMAGES

JOB 233
DR. AJF
DATE 1-4-54
CK.
DATE
SCALE
MAT'L
SIZE
A-5462

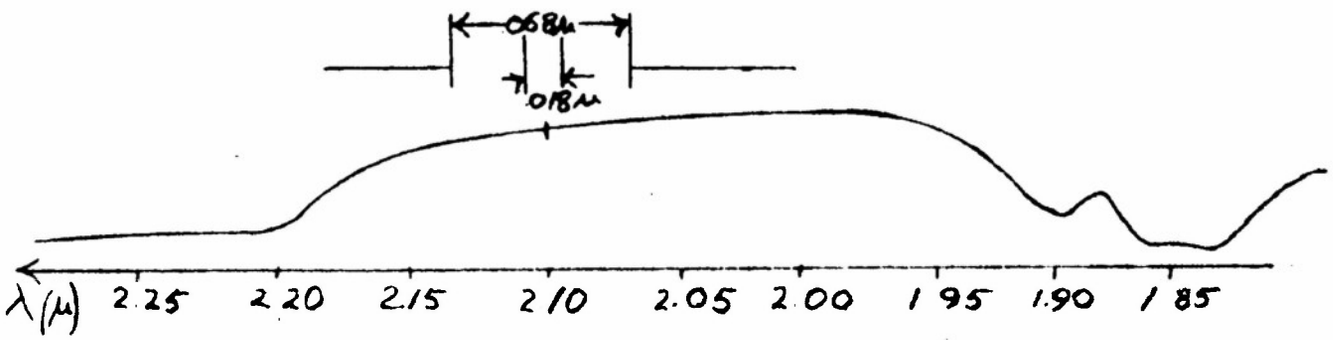

FIG. 9

SLITWIDTH AND ABSORPTION BANDS

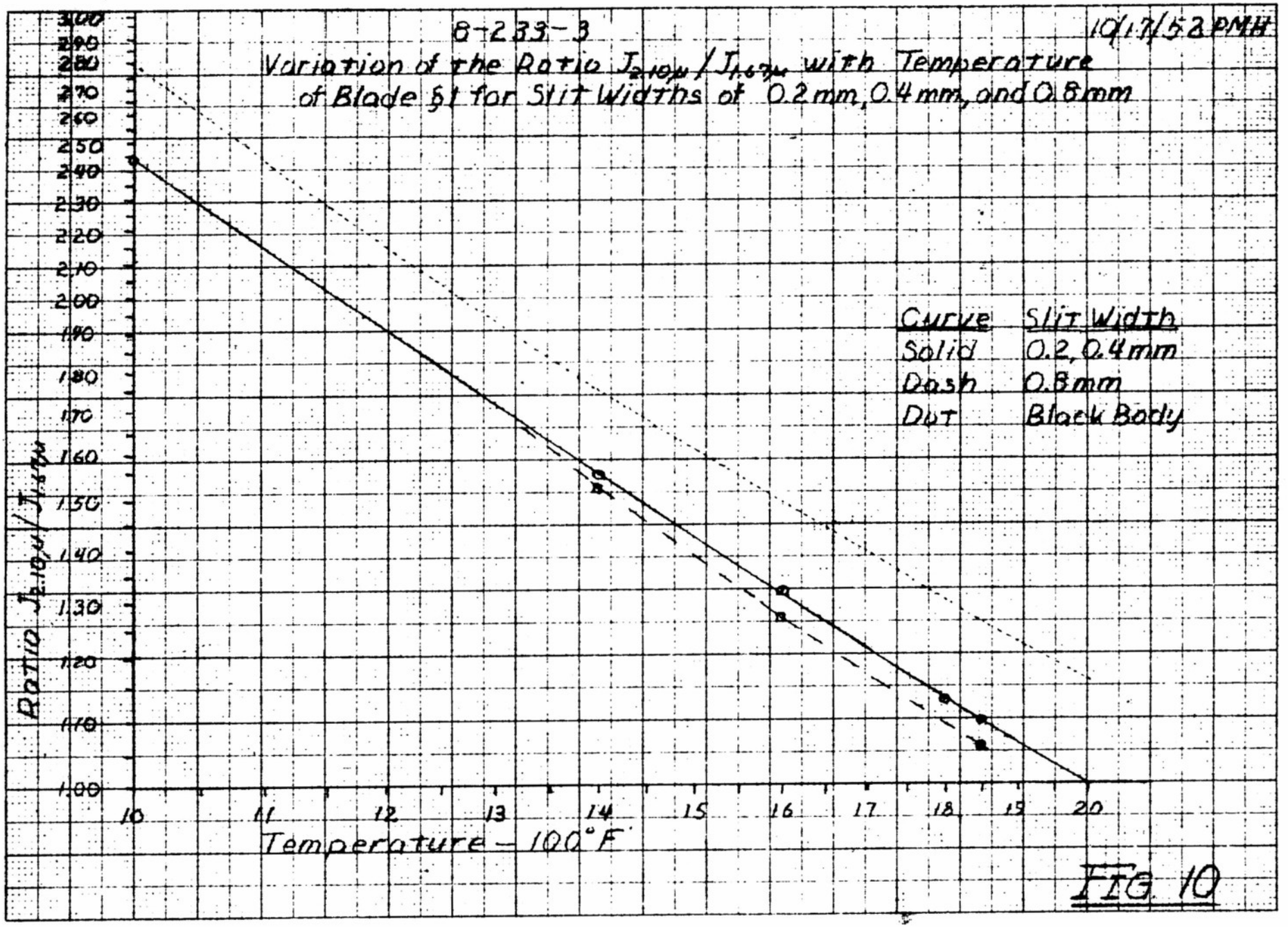

FIG. 10

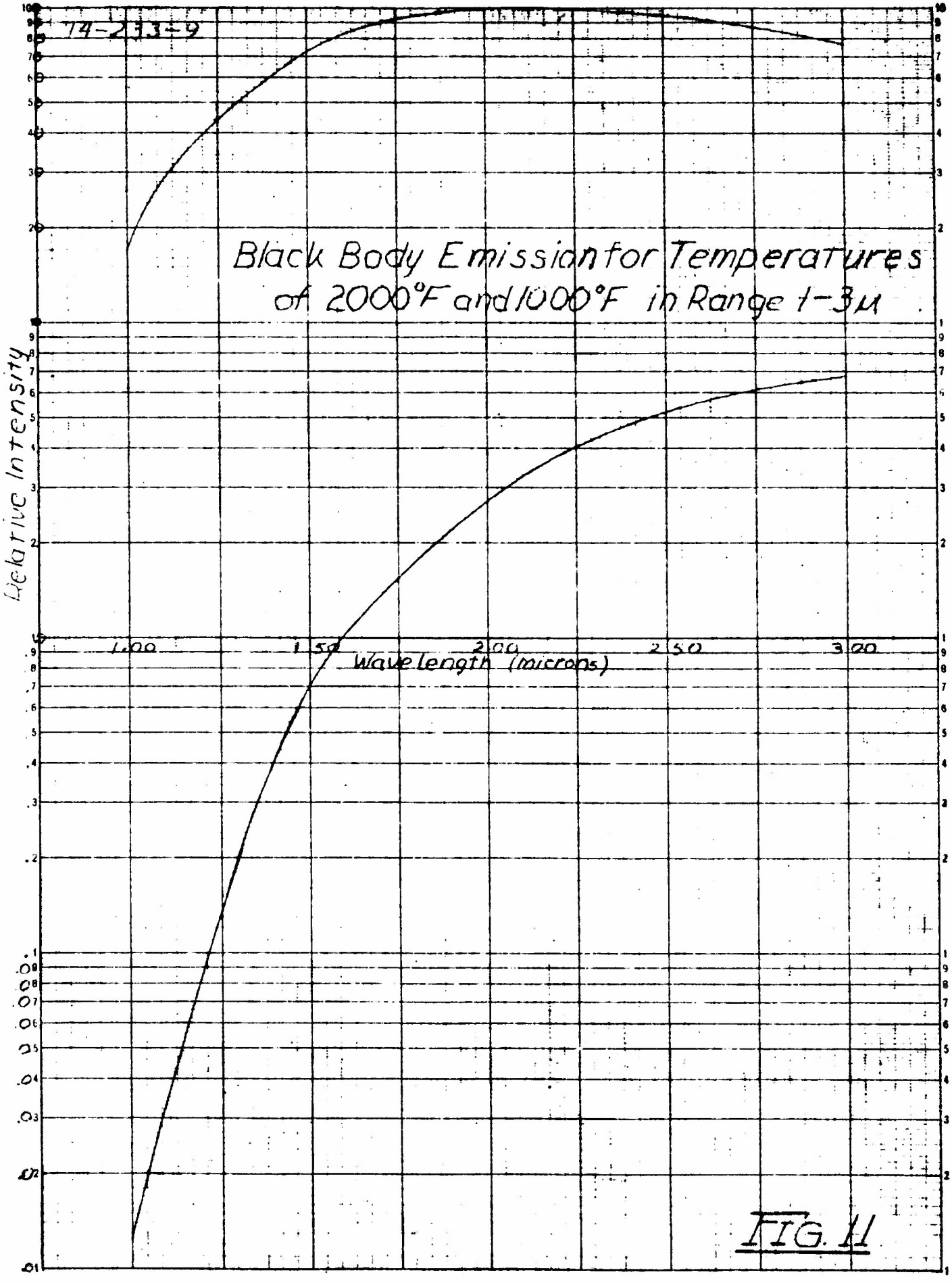
74-233-9
Black Body Emission for Temperatures of 2000°F and 1000°F in Range 1-3μ
Relative Intensity
1.00
1.50
2.00
2.50
3.00
Wavelength (microns)

FIG. 11

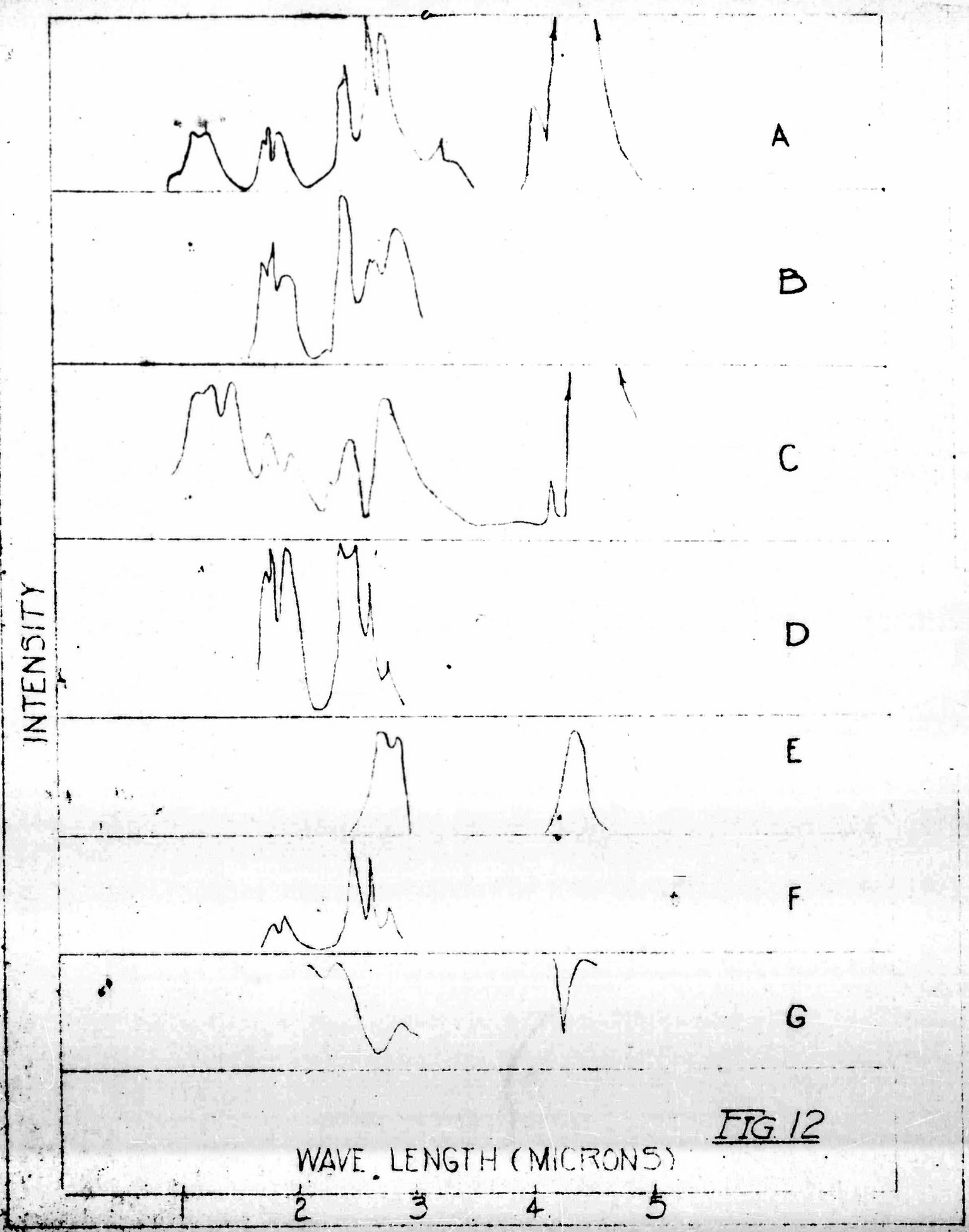

FIG 12

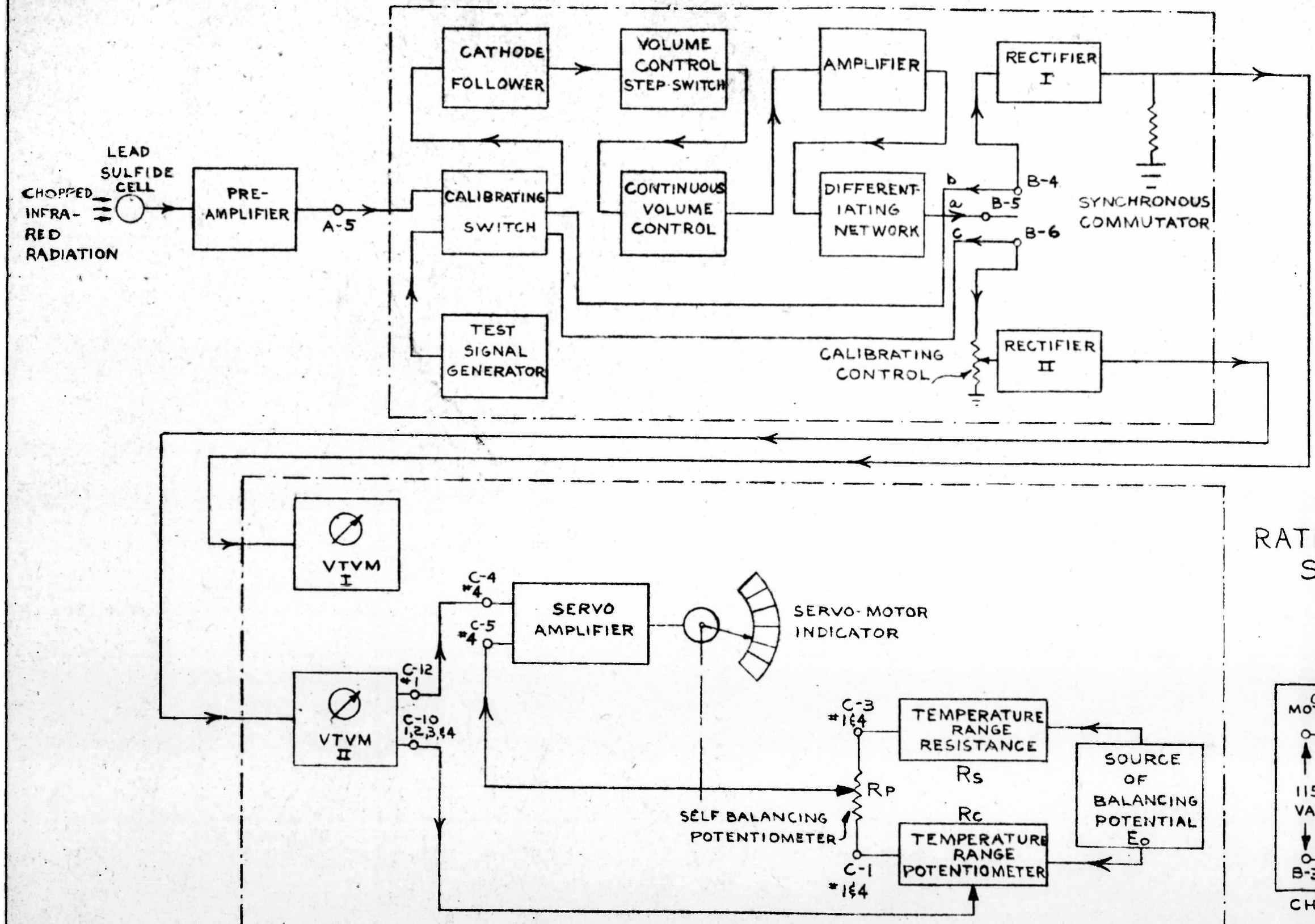

AMPLIFIER SECTION

RATIO-CIRCUIT SECTION

FIG. 13

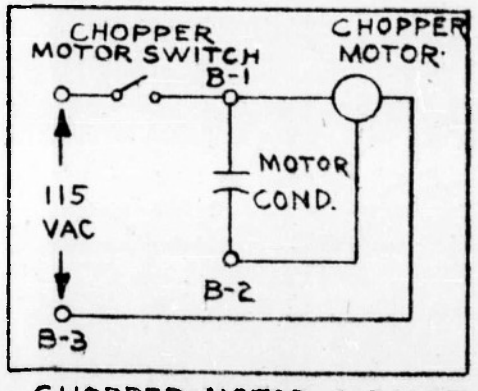

CHOPPER-MOTOR CIRCUIT

No.	CHANGE	BY	DATE
4			
3			
2			
1			

INDUSTRIAL SCIENTIFIC COMPANY
84 W. 33 ST.
NEW YORK 1, N. Y.

MACH. DICHROMATIC PYROMETER
ASS'Y.
PART BLOCK DIAGRAM

JOB 233
DR. REL
DATE 1-5-54
CK.
DATE
SCALE NONE
MAT'L
SIZE
B-2259

June 9, 1953

9-233-4

Dichromatic Pyrometer
Temperature Calibration Curve

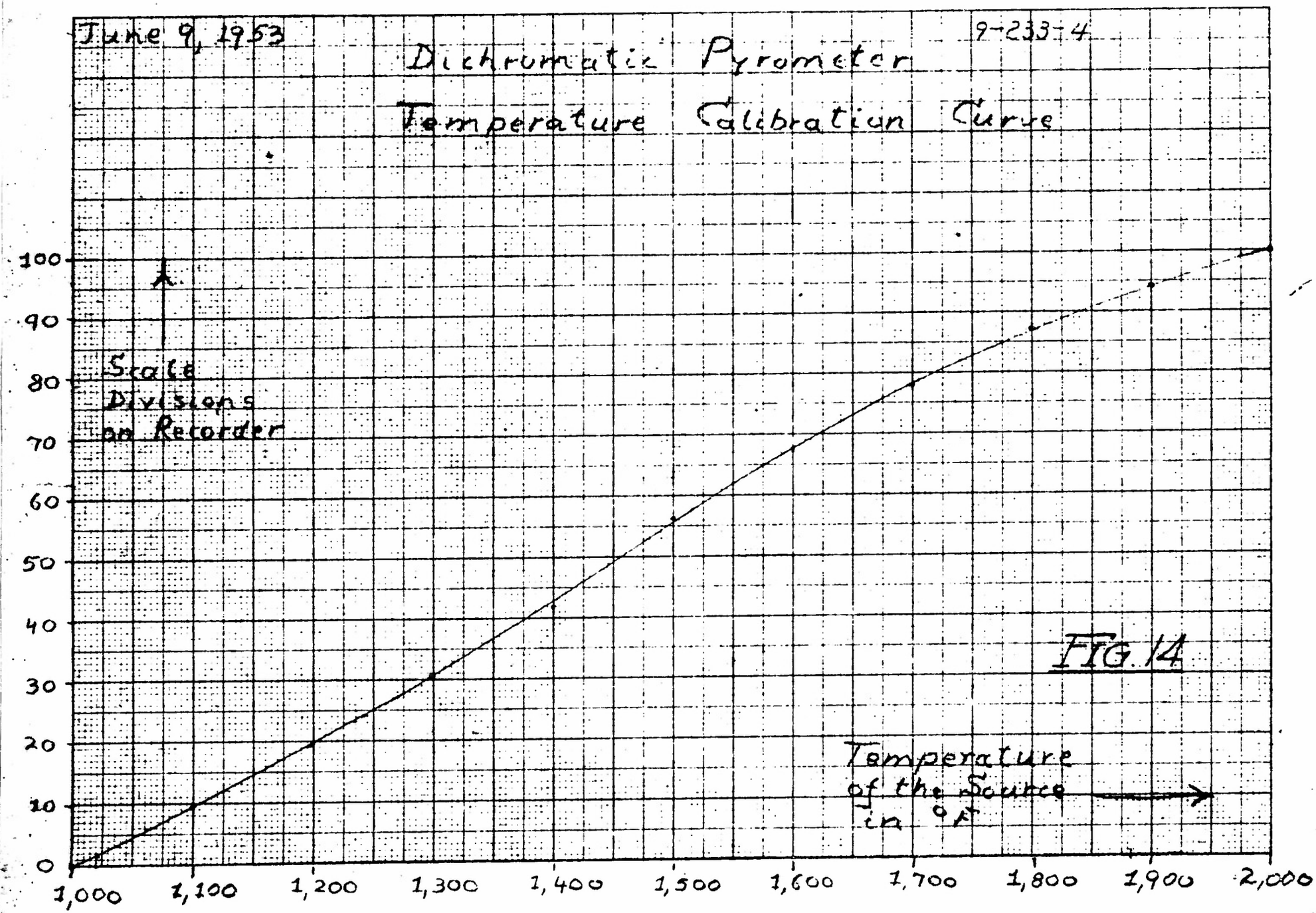

FIG. 14

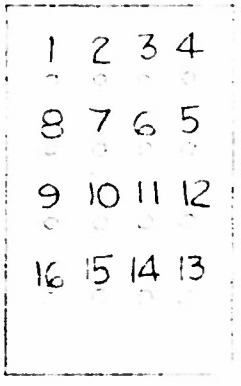

FIG 15

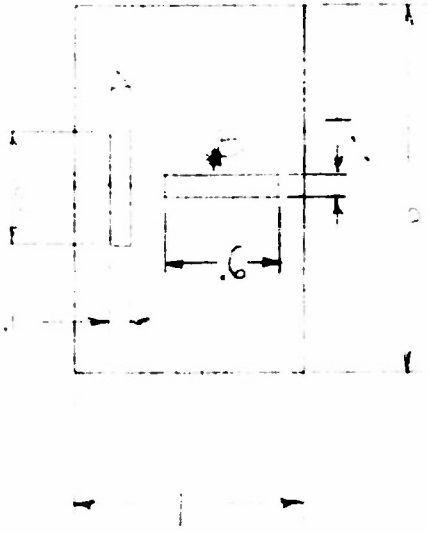

FIG. 17

No.	CHANGE	BY	DATE
4			
3			
2			
1			

9			
8			
7			
6			
5			

INDUSTRIAL SCIENTIFIC COMPANY
34 W. 33 ST.
NEW YORK 1, N. Y.

MACH. DICHROMATIC PYROMETER
ASS'Y.
PART ARRGT OF TARGET AREA & THERMOCOUPLES

JOB 233
DR. AJF
DATE 1/5/54
CK.
DATE
SCALE
MAT'L
SIZE A5466

15-17

10-233-5

Tests at AEL July 1953
Thermocouple Gradients
$\Delta T = T_{14} - T_{13}$
$T = \frac{T_{14} + T_{13}}{2}$

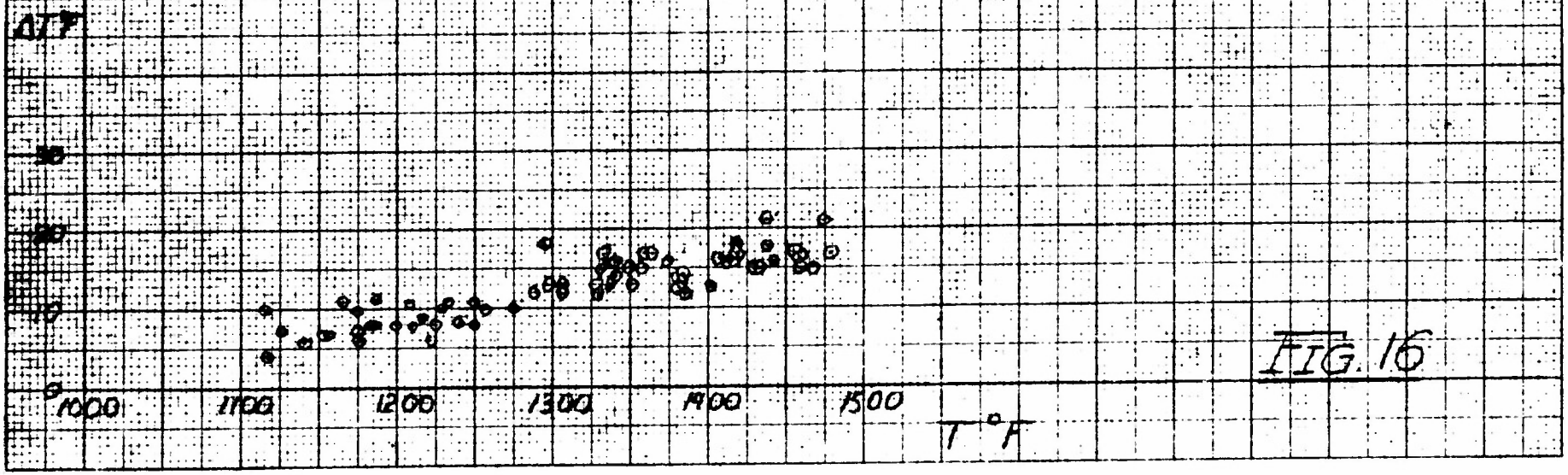

FIG. 16

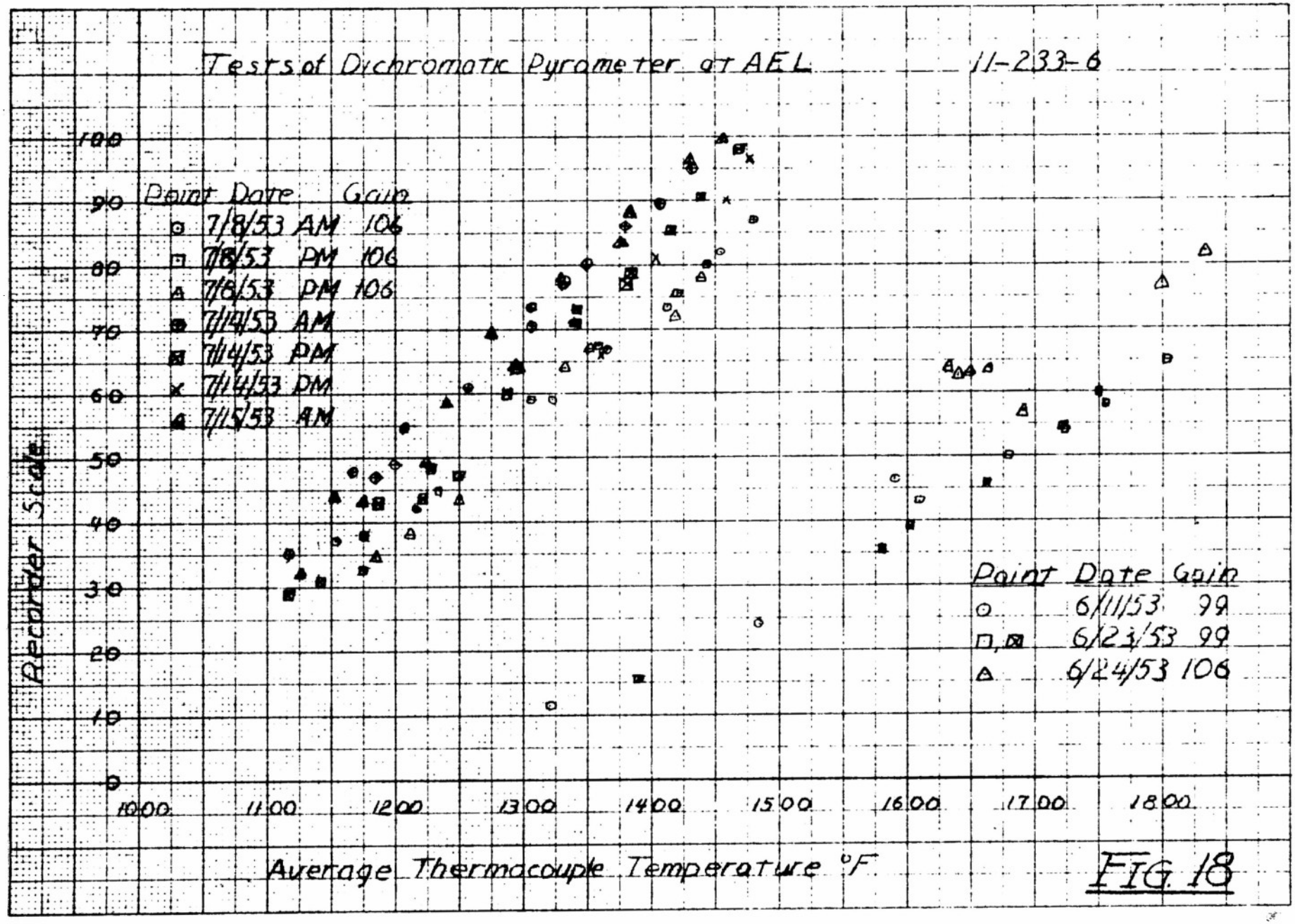

FIG 18

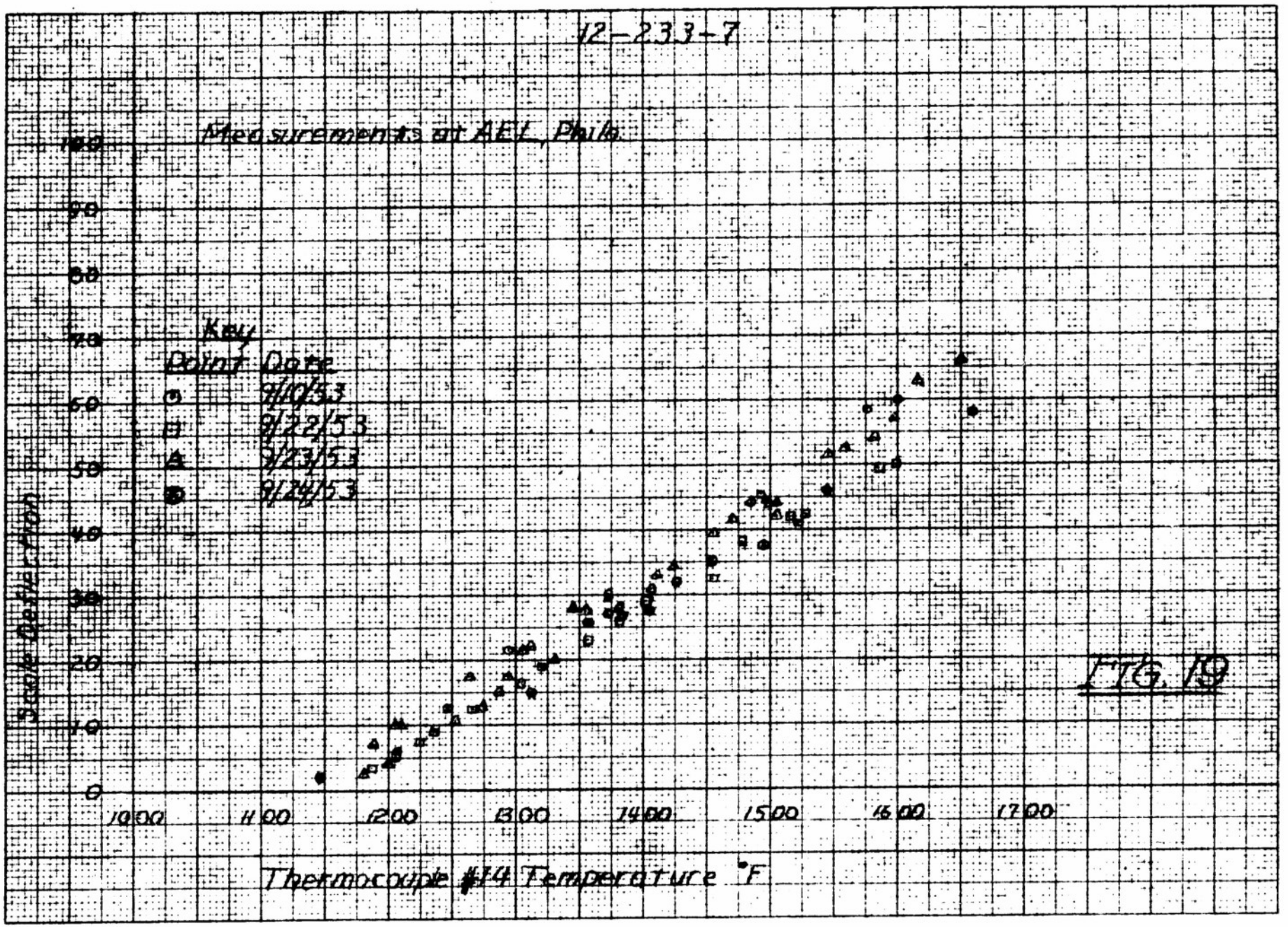

FIG. 19

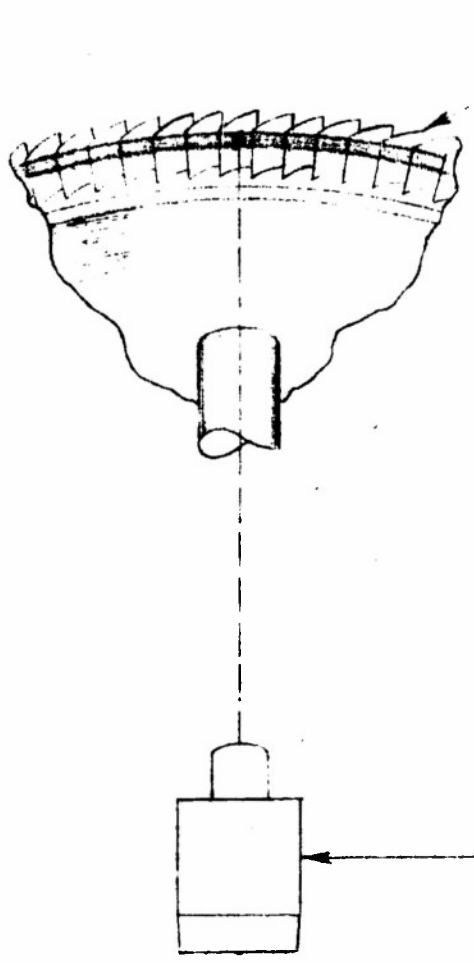

FIG. 20

No.	CHANGE	BY	DATE
4			
3			
2			
1			

9			
8			
7			
6			
5			

INDUSTRIAL SCIENTIFIC COMPANY
34 W. 33 ST.
NEW YORK 1, N. Y.

MACH. DICHROMATIC PYROMETER
ASS'Y. APPLICATION TO
PART TURBINE BLADES

JOB
JOB
JOB
JOB
JOB
JOB 233
D.R.
DATE
CK.
DATE
SCALE
MAT'L
SIZE
A 5592

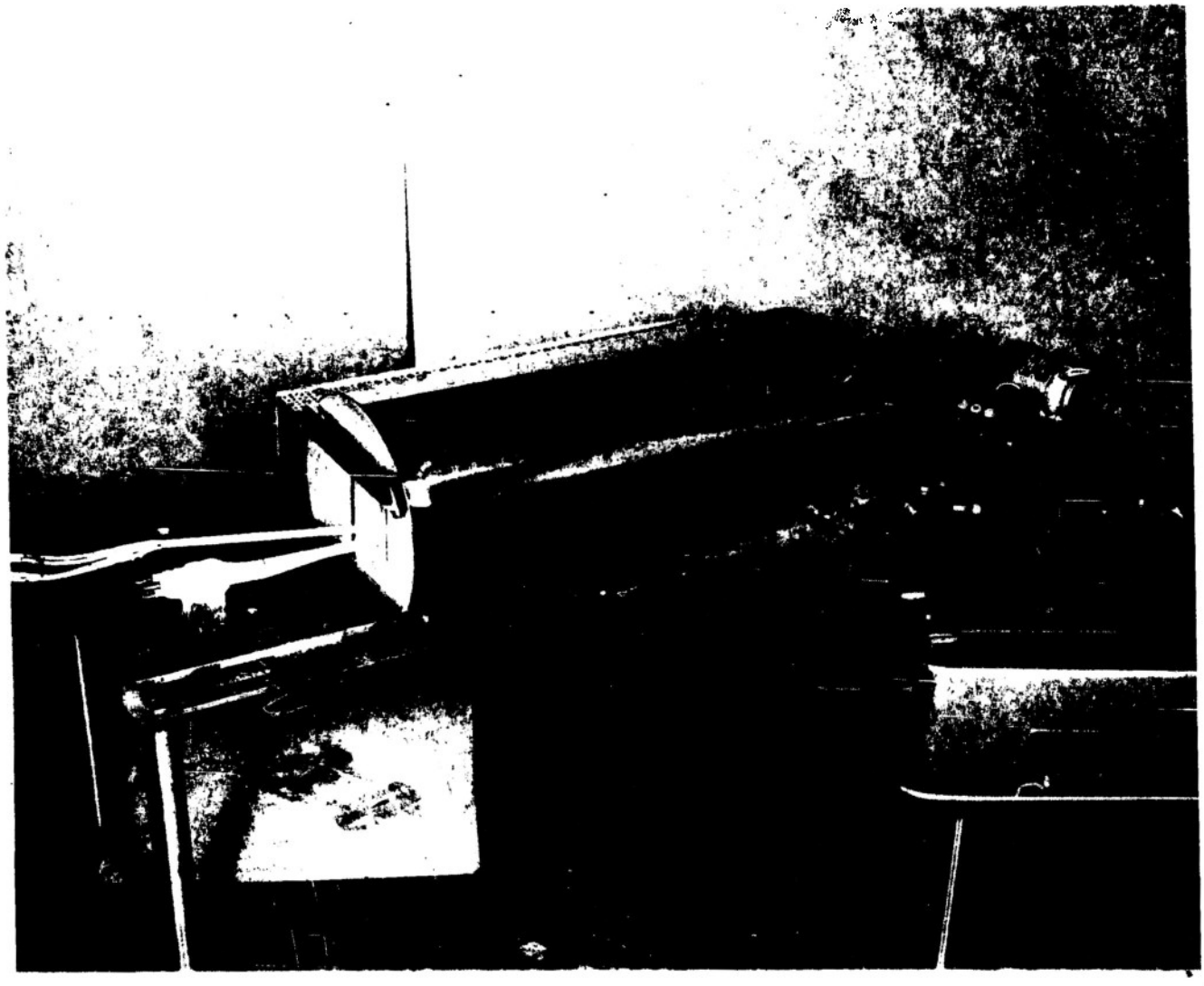

FIG. 21 VIEW OF SETUP USED FOR MEASURING TURBINE BLADE EMISSIVITIES.

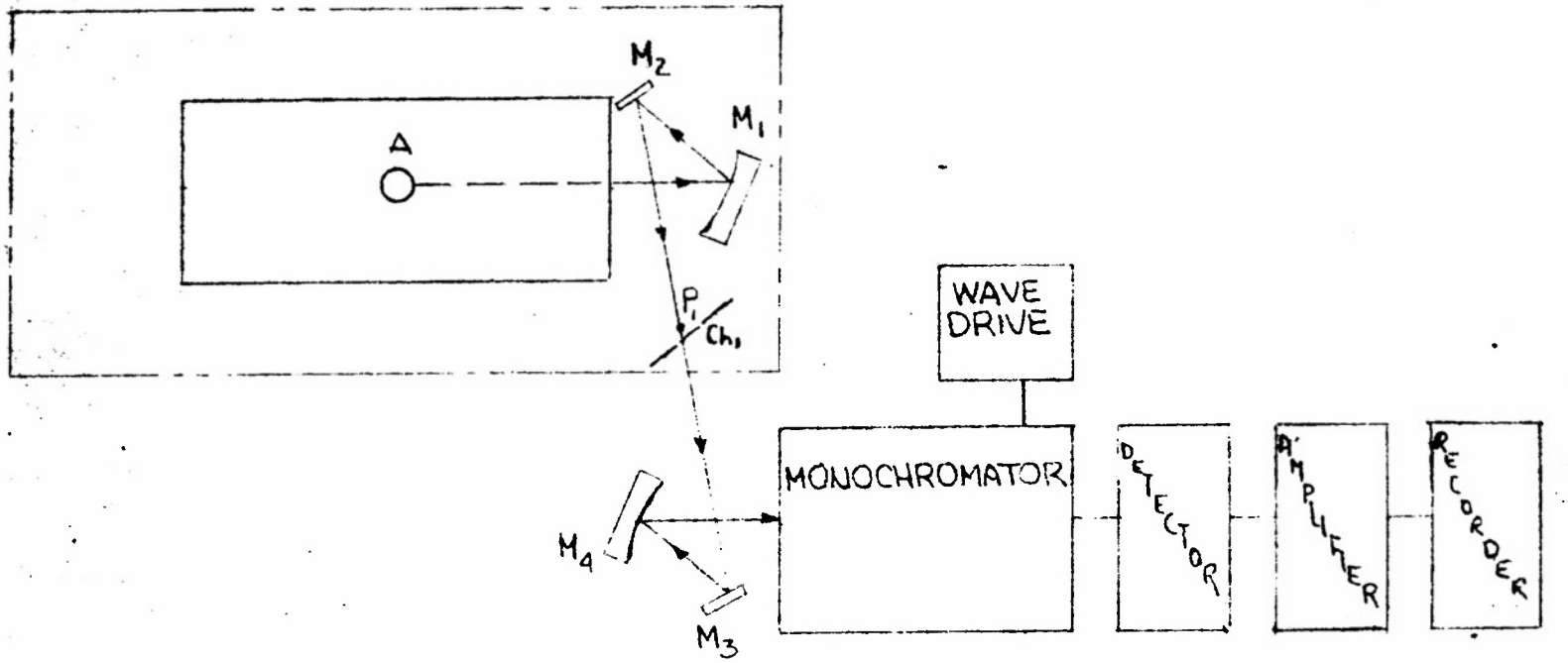

FIG 22

4				9				INDUSTRIAL SCIENTIFIC COMPANY 34 W. 33 ST. NEW YORK 1, N. Y.	MACH. EMISSIVITY MEASUREMENTS
3				8					ASS'Y. LABORATORY SETUP
2				7					PART
1				6					
No.	CHANGE	BY	DATE	5					

JOB
JOB
JOB
JOB
JOB
JOB 233

DR. AJF
DATE 4-5-54
CK.
DATE
SCALE
MAT'L -
SIZE
H5463

FIG. 23 SAMPLES OF TURBINE BLADE MATERIALS AND BLACKBODY TARGETS.

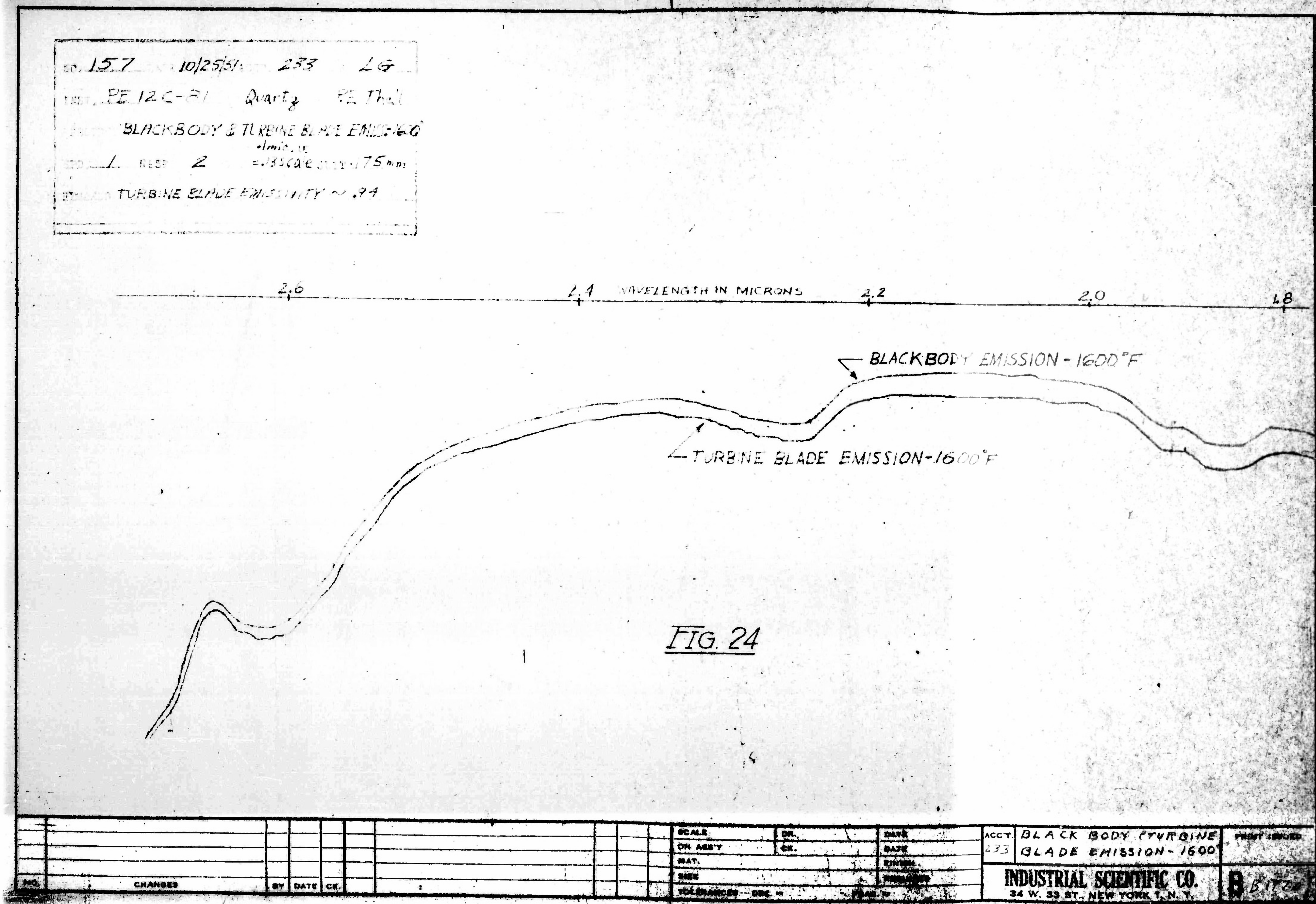
157 10/25/51 233 LG
PE 12 C-81 Quartz PE Thai
BLACKBODY & TURBINE BLADE EMISS 1600
TURBINE BLADE EMISSIVITY ~ .94
2.6
2.4
WAVELENGTH IN MICRONS
2.2
2.0
1.8
BLACKBODY EMISSION - 1600°F
TURBINE BLADE EMISSION-1600°F
BLACK BODY & TURBINE BLADE EMISSION - 1600
INDUSTRIAL SCIENTIFIC CO.
34 W. 33 ST. NEW YORK 1, N. Y.

FIG. 24

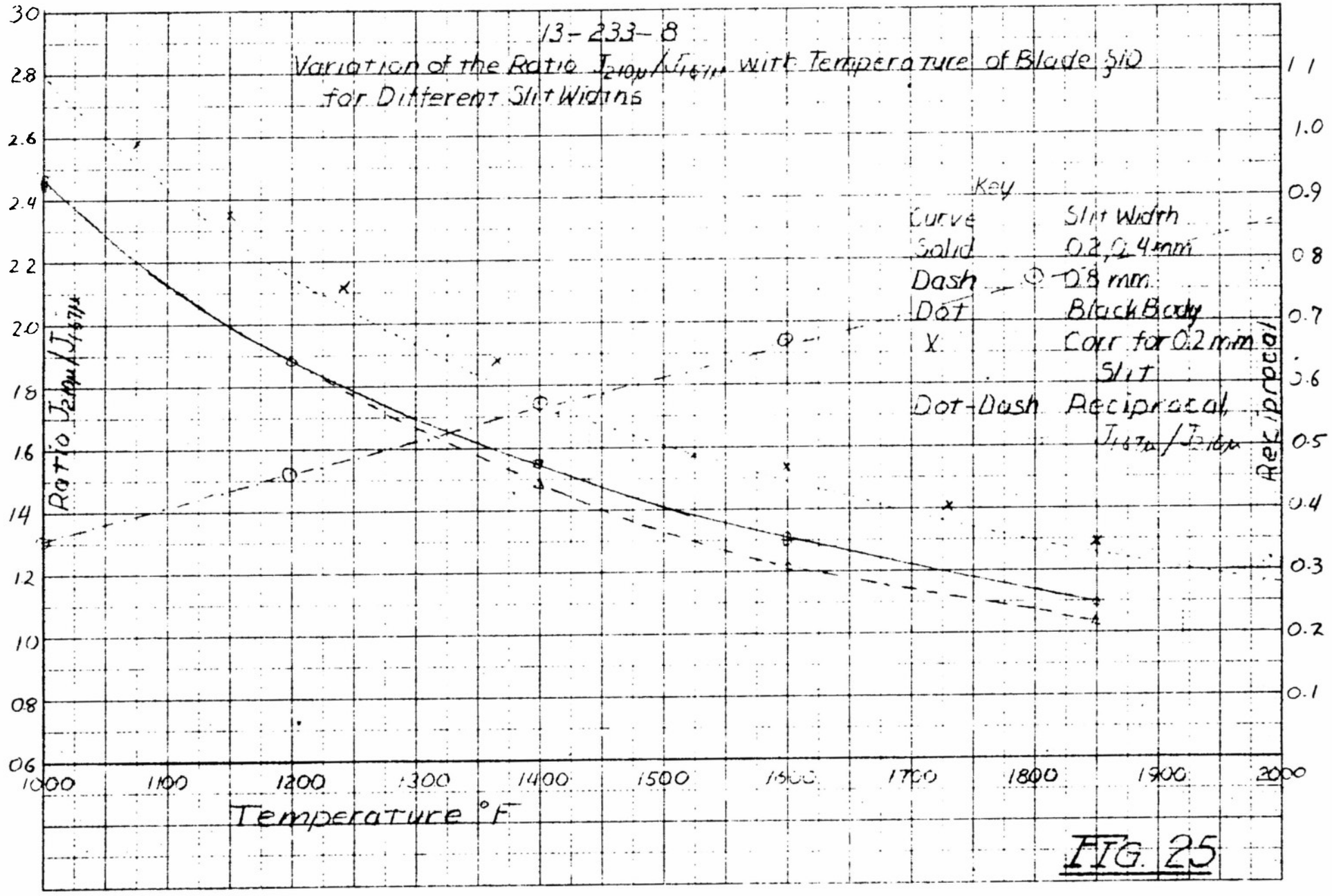
13-233-8
Variation of the Ratio $I_{2\mu}/I_{1.67\mu}$ with Temperature of Blade 510
for Different Slit Widths
Key
Curve
Solid
Dash
Dot
X
Dot-Dash
Slit Width
0.2, 0.4 mm
0.8 mm
Black Body
Corr for 0.2 mm Slit
Reciprocal $I_{1.67\mu}/I_{2\mu}$
Ratio $I_{2\mu}/I_{1.67\mu}$
Reciprocal
Temperature °F
30
2.8
2.6
2.4
2.2
2.0
1.8
1.6
1.4
1.2
1.0
0.8
0.6
1.1
1.0
0.9
0.8
0.7
0.6
0.5
0.4
0.3
0.2
0.1
1000
1100
1200
1300
1400
1500
1600
1700
1800
1900
2000

FIG. 25

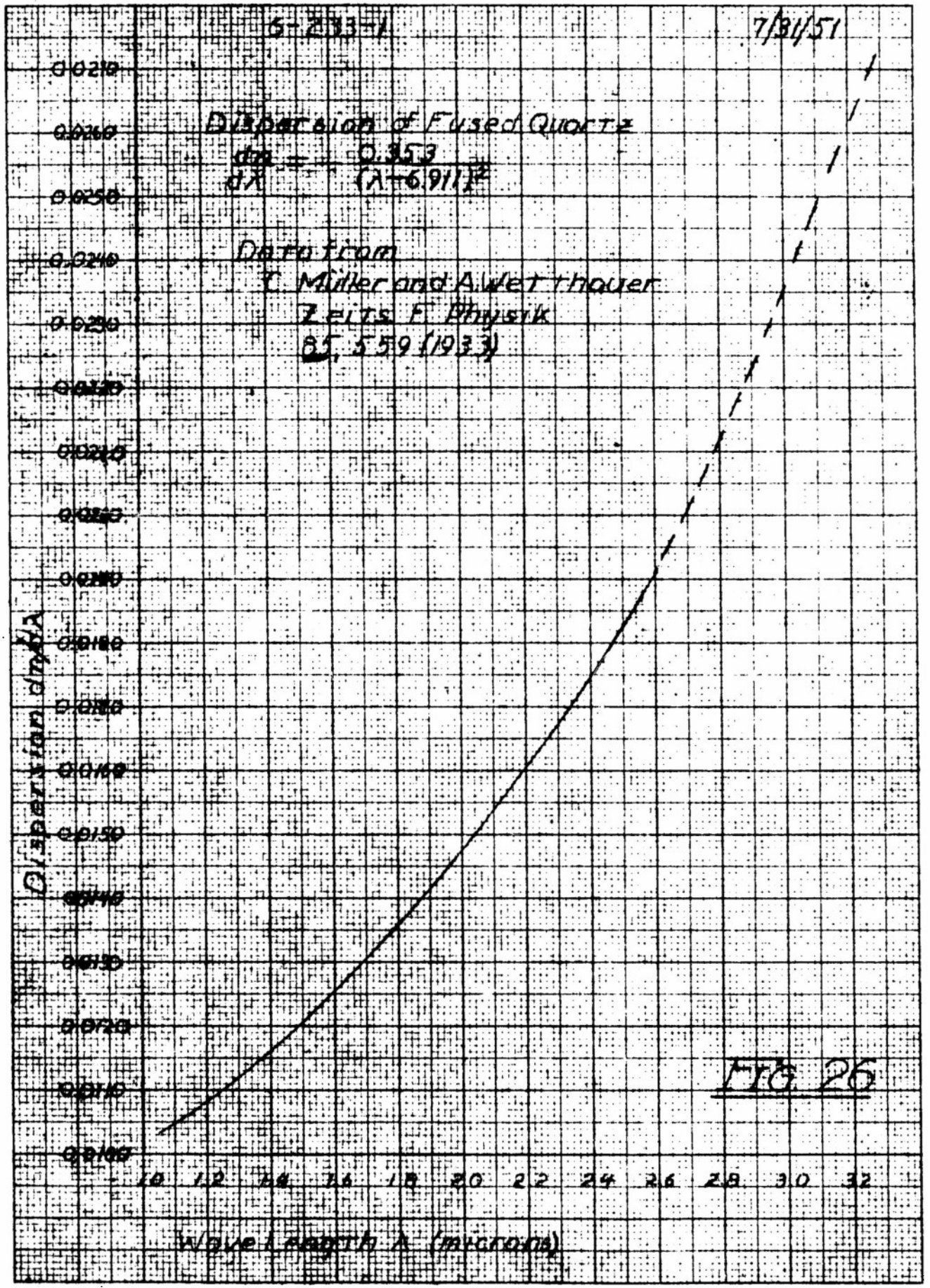

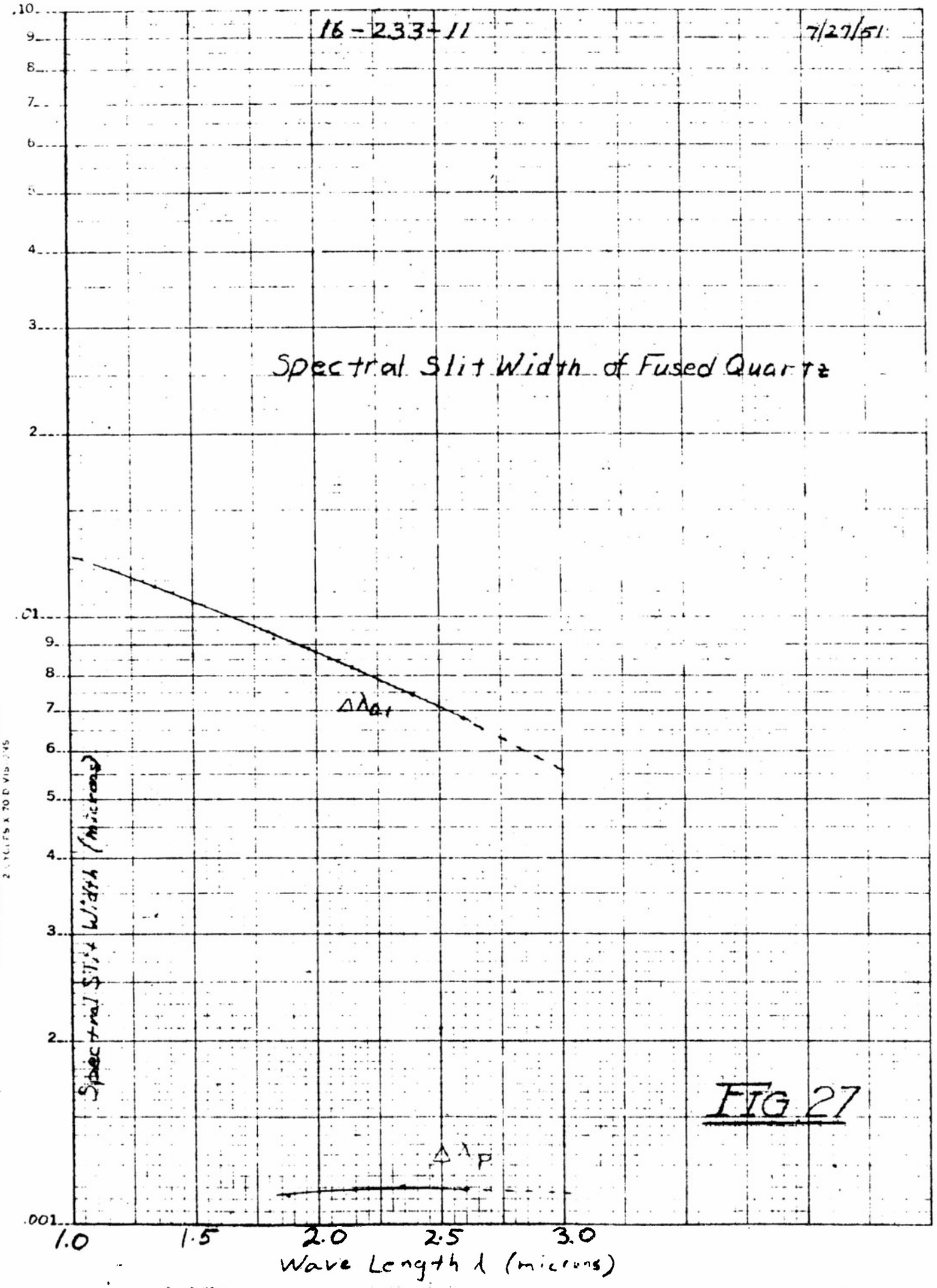
16-233-11
7/27/51
Spectral Slit Width of Fused Quartz
Spectral Slit Width (Microns)
Wave Length λ (microns)
$\Delta\lambda_a$
$\Delta\lambda_p$
10
9
8
7
6
5
4
3
2
.01
9
8
7
6
5
4
3
2
.001
1.0
1.5
2.0
2.5
3.0
K&E SEMI LOGARITHMIC 359-61
KEUFFEL & ESSER CO.

FIG 27

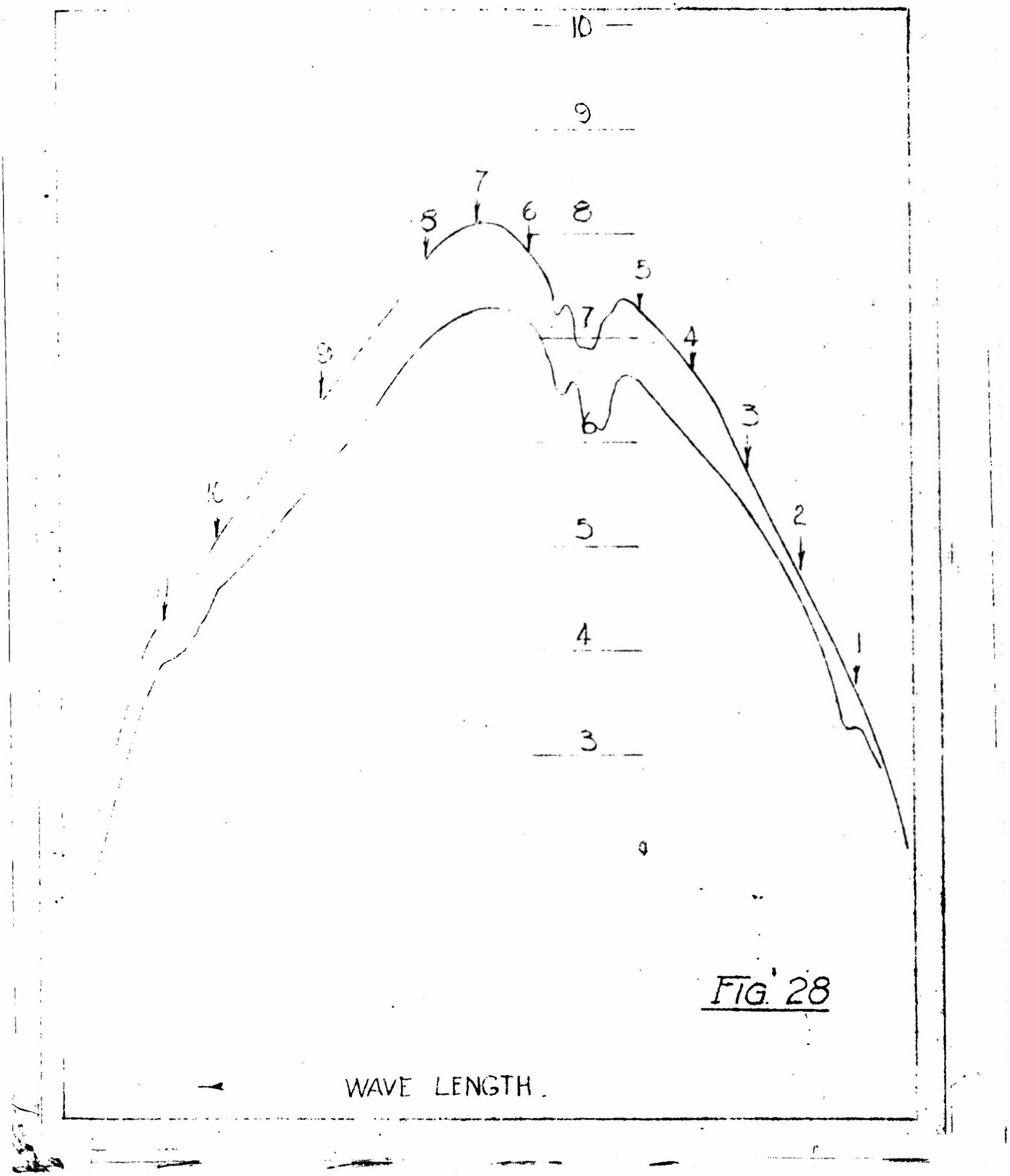

FIG. 28

BINDING SPACE

FIG. 29

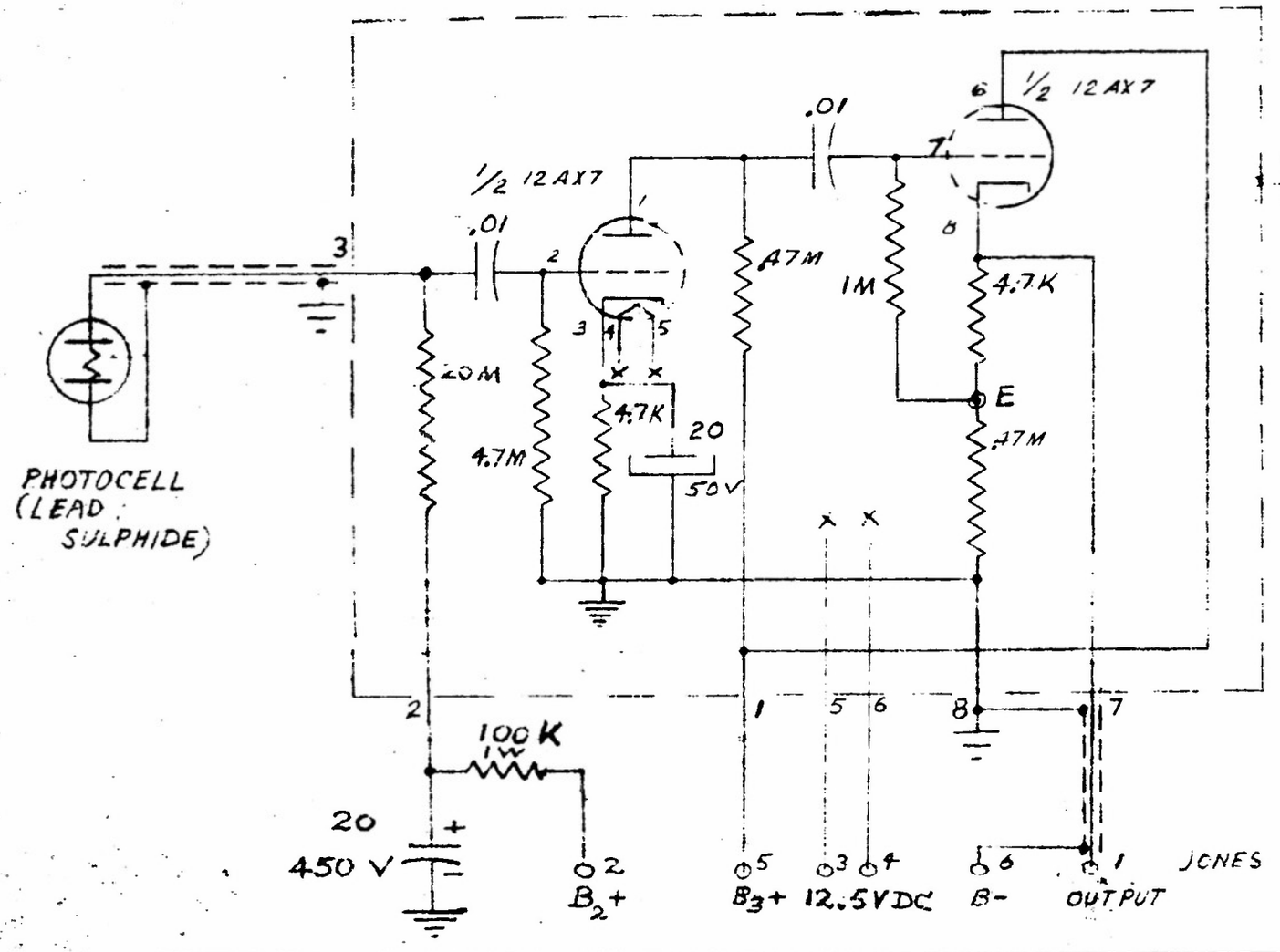

NO.	CHANGES	BY	DATE	CK.

SCALE | DR R.E. KRAUS | DATE 3-9-52
ON ASS'Y | CK | DATE
MAT. | FINISH
SIZE | REQUIRED
TOLERANCES -- DEC. ± | FRAC. ±

ACCT. 233

PREAMPLIFIER
SCHEM. CIRCUIT DIAG.

INDUSTRIAL SCIENTIFIC CO.
34 W. 33 ST., NEW YORK 1, N.Y.

PRINT ISSUED

A4559

FIG. 30

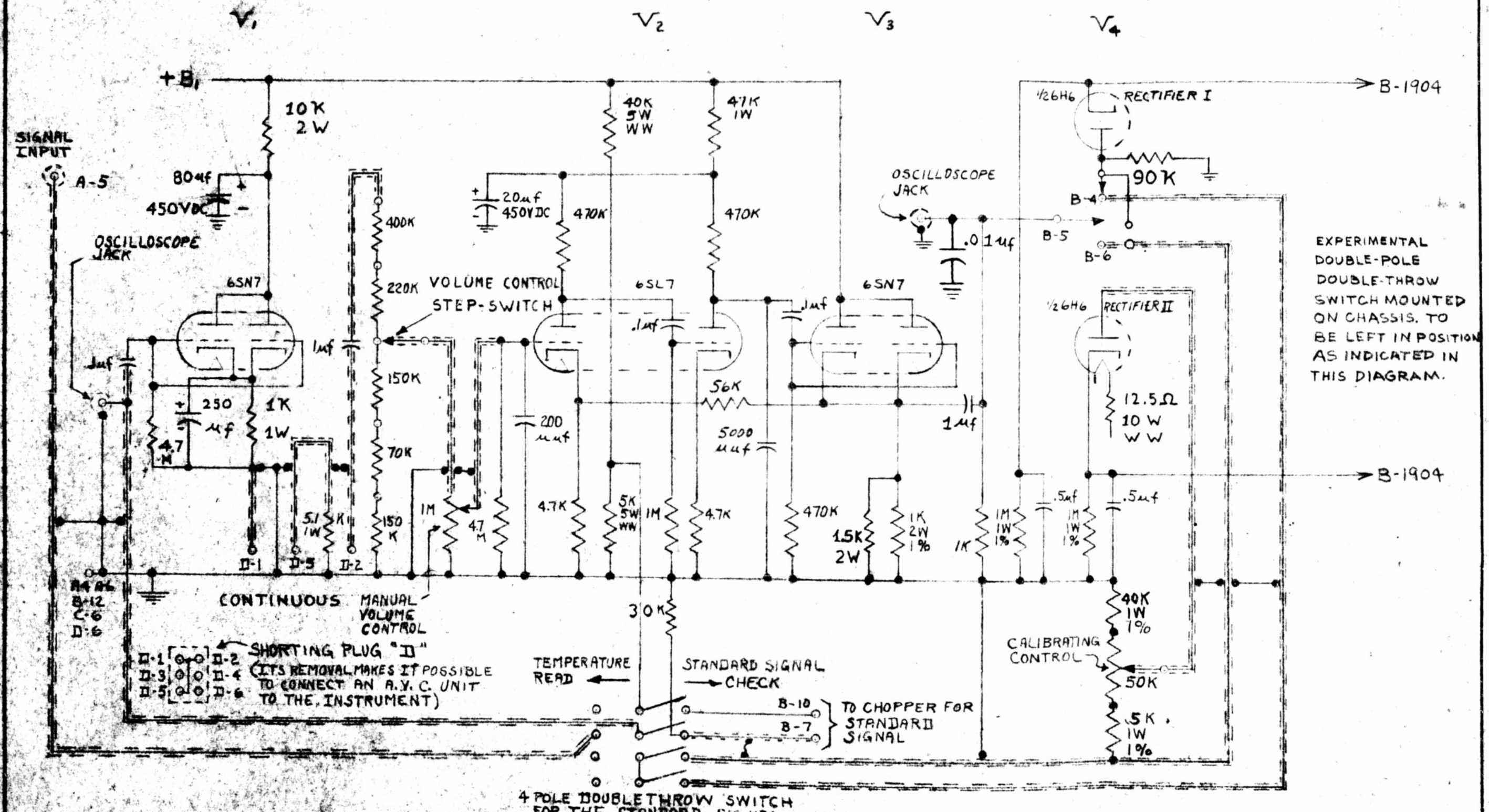

EXPERIMENTAL DOUBLE-POLE DOUBLE-THROW SWITCH MOUNTED ON CHASSIS. TO BE LEFT IN POSITION AS INDICATED IN THIS DIAGRAM.

NO.	CHANGES	BY	DATE	CK.

SCALE NTS	DR. C CASTRO	DATE 6/5/53	ACC'T. 233
ON ASS'Y	CK.	DATE	DICHROMATIC PYROMETER AMPLIFIER CKT. DIAGRAM
MAT.		FINISH	PRINT ISSUED
SIZE		REQUIRED	INDUSTRIAL SCIENTIFIC CO. 34 W. 33 ST., NEW YORK 1, N. Y.
TOLERANCES ~ DEC.=	FRAC.=		B-2000

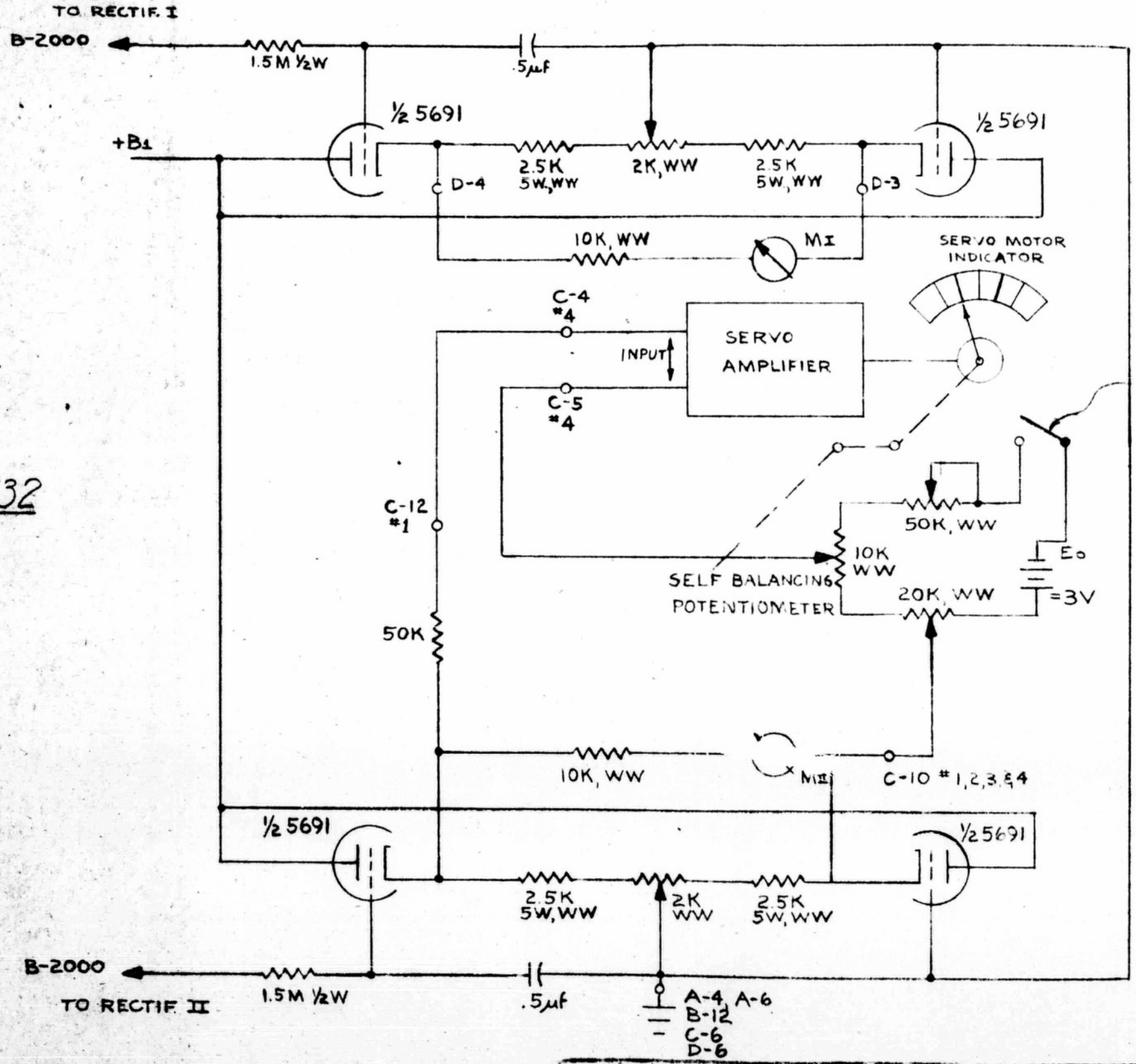

V5

V6

FIG. 32

NOTE:
ALL CONNECTIONS TO PLUG "C" SHOWN ON THIS DIAGRAM ARE GOING TO THE CORRESPONDING PRONG NUMBERS OF PLUG C#1 ON DWG. B-2002.

No.	CHANGE	DATE
4		
3		
2		
1		

INDUSTRIAL SCIENTIFIC COMPANY 34 W. 33 ST. NEW YORK 1, N. Y.

DICHROMATIC PYROMETER

ASS'Y.

PART RATIO CIRCUIT DIAGRAM

JOB 233

REL

DATE 1-4-54

CK.

DATE

SCALE NONE

MAT'L

SIZE B-2258

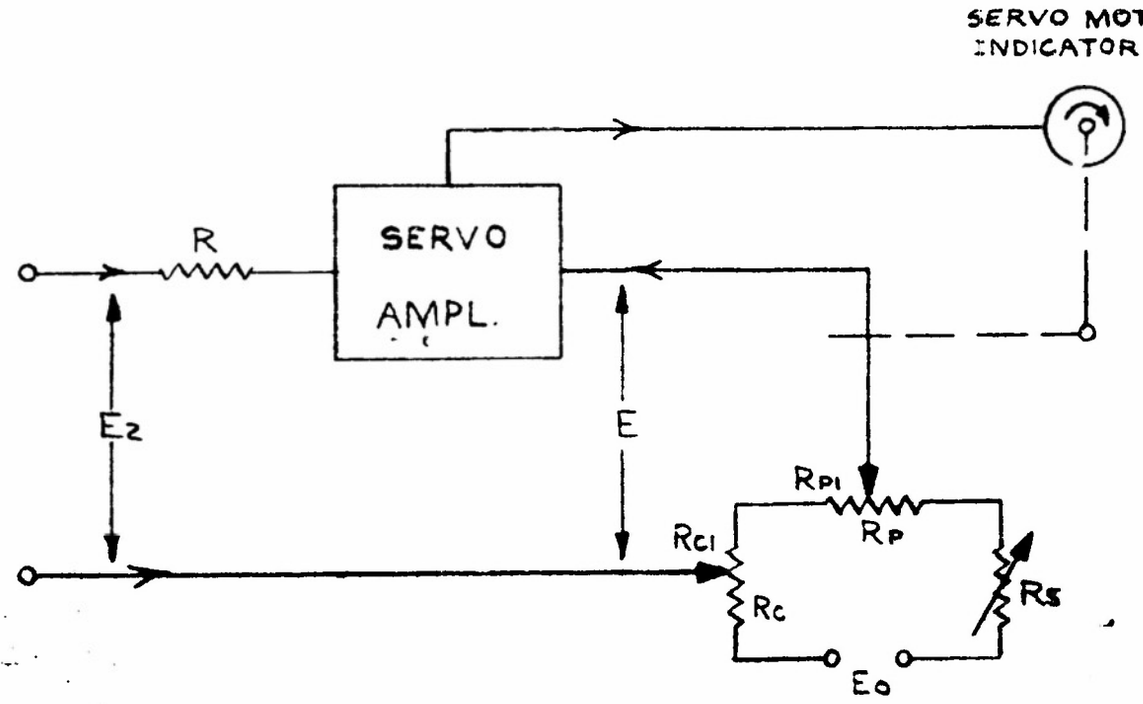

FIG. 33

4				9				INDUSTRIAL SCIENTIFIC COMPANY 34 W. 33 ST. NEW YORK 1, N. Y.	MACH. DICHROMATIC PYROMETER	
3				8					ASS'Y.	
2				7					PART SIMPLIFIED RATIO CIRCUIT	A-S470
1				6						
No.	CHANGE	BY	DATE	5						

JOB
JOB
JOB
JOB
JOB 239
DR. REL
DATE 1-4-54
CK.
DATE
SCALE NONE
MAT'L
SIZE

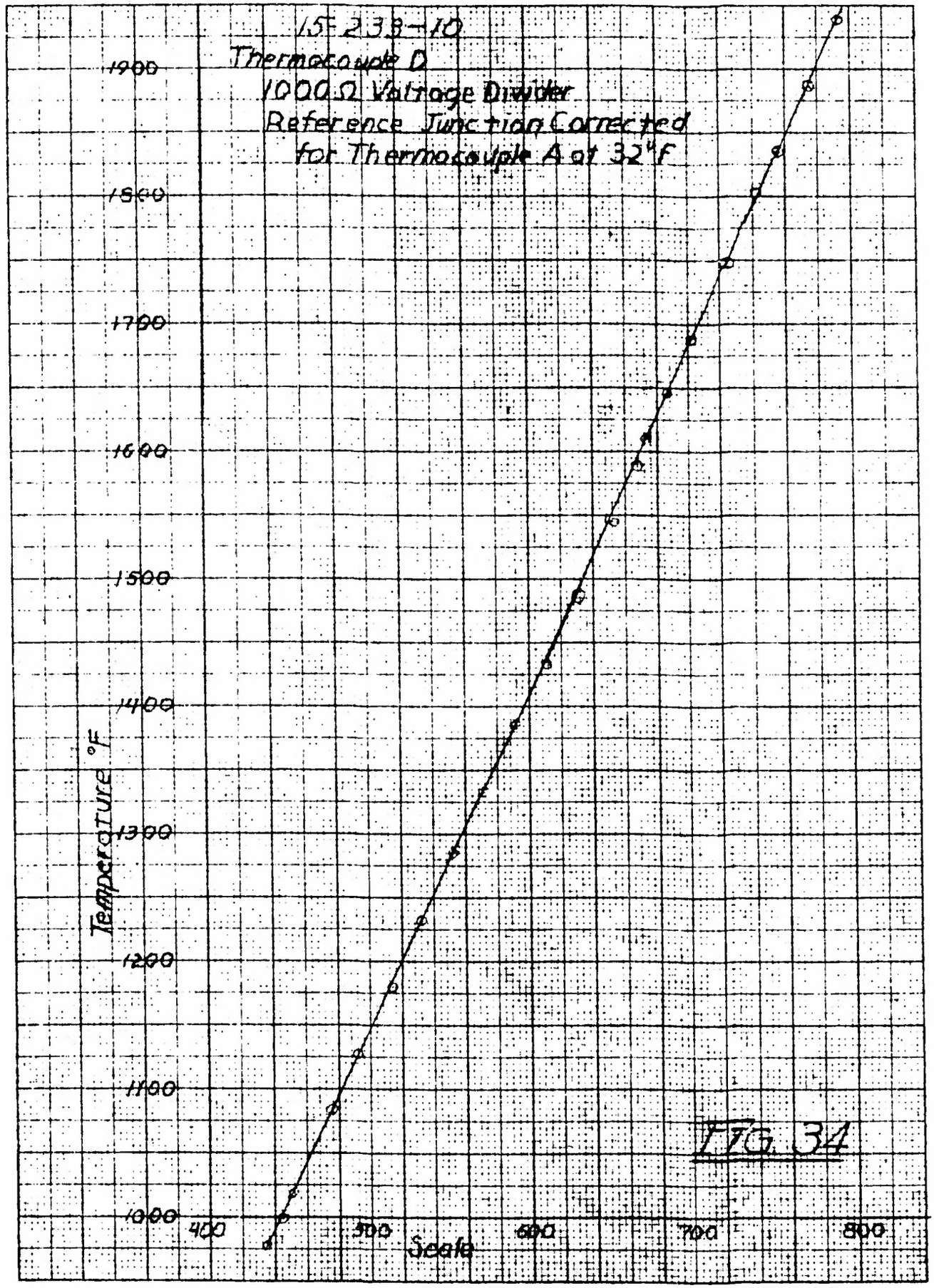

FIG. 34

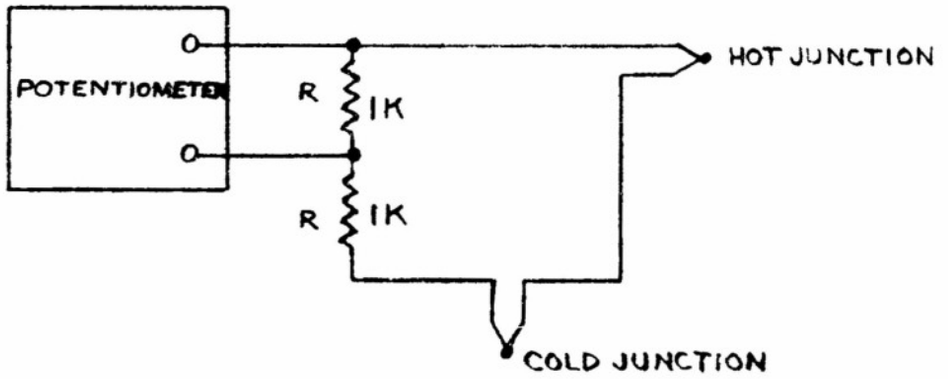

FIG. 35

No.	CHANGE	BY	DATE
4			
3			
2			
1			

9								
8								
7								
6								
5								

INDUSTRIAL SCIENTIFIC COMPANY
34 W. 33 ST.
NEW YORK 1, N. Y.

MACH. DICHROMATIC PYROMETER
ASS'Y.
PART THERMOCOUPLE MEASURING CIRCUIT

JOB
JOB
JOB
JOB 233
DR. REL
DATE 1-5-54
CK.
DATE
SCALE NONE
MAT'L
SIZE
A-5471